Picosecond absorption spectroscopy of self-trapped excitons and transient Ce states in $LaBr_3$ and $LaBr_3$:Ce

Peiyun Li, Sergii Gridin, K. Burak Ucer, and Richard T. Williams*
Department of Physics, Wake Forest University, Winston Salem, North Carolina 27106, USA

Peter R. Menge
Saint-Gobain Crystals, 17900 Great Lakes Parkway, Hiram, Ohio 44234, USA

(Received 1 March 2018; revised manuscript received 29 March 2018; published 18 April 2018)

Picosecond time-resolved optical absorption spectra induced by two-photon interband excitation of $LaBr_3$ are reported. The spectra are similar in general characteristics to self-trapped exciton (STE) absorption previously measured in alkali halides and alkaline-earth halides. A broad ultraviolet absorption band results from excitation of the self-trapped hole within the STE. A series of infrared and red-visible bands results from excitation of the bound outer electron within the STE similar to bands found in alkali halides corresponding to different degrees of "off-center" relaxation. Induced absorption in cerium-doped $LaBr_3$ after band-gap excitation of the host exhibits similar STE spectra, except it decays faster on the tens-of-picoseconds scale in proportion to the Ce concentration. This is attributed to dipole-dipole energy transfer from STE to Ce^{3+} dopant ions. The absorption spectra were also measured after direct excitation of the Ce^{3+} ions with sufficient intensity to drive two- and three-photon resonantly enhanced excitation. In this case, the spectrum attributed to STEs created adjacent to Ce^{3+} ions decays in 1 ps suggesting dipole-dipole transfer from the nearest-neighbor separation. A transient absorption band at 2.1 eV growing with Ce concentration is found and attributed to a charge-transfer excitation of the Ce^{3+*} excited state responsible for scintillation in $LaBr_3$:Ce crystals. This study concludes that the energy transport from host to activator responsible for the scintillation of $LaBr_3$:Ce proceeds by STE creation and dipole-dipole transfer more than by sequential trapping of holes and electrons on Ce^{3+} ions.

DOI: 10.1103/PhysRevB.97.144303

I. INTRODUCTION

Lanthanum halide crystals with the formula LaX_3 comprise the trihalide member of a progression of binary metal halide crystalline compounds in which both cations and anions have closed p shells similar to rare-gas atoms. The simplest structures are the alkali halides, AX, then alkaline-earth halides, $(AE)X_2$, and then lanthanum halides, LaX_3. $LaBr_3$, in particular, is the topic of this study. All have fairly wide transparency gaps and, among other applications, the three material groups have been found to make good hosts for luminescence and scintillation when suitably doped. Their "hard sphere" ions with closed p shells are pulled or pushed as tightly against each other as ion sizes allow in the crystal ground state. Things change dramatically upon removal of a p-shell electron from halide ions comprising the top of the valence band in all three of the considered compound classes. Valence electron removal may be viewed as creating a highly reactive open-shell halogen atom which relaxes to localize the hole in a bond with a neighboring halide ion. Känzig first discovered the V_k center or self-trapped hole (STH) in alkali halides [1], comprising a diatomic halide molecular ion pair localizing a valence hole, and symmetrically situated about the mid-point of the halide pair in the perfect lattice. Other examples of STH are found in various crystals, most commonly metal halides [2].

When an excited electron is bound to the STH, the resulting self-trapped exciton (STE) exhibits transient optical absorption in the ultraviolet that is similar to the stable V_k spectrum and is often described as a hole transition of the STE involving mainly molecular orbitals of the bonded halide pair [3]. The STE also exhibits infrared or visible transitions of the more loosely bound outer electron, the so-called electron transitions of the STE. The STE relaxed lattice configuration may or may not preserve the same symmetric disposition and orientation of the STH (V_k center). STE excited states have been studied by transient optical absorption spectroscopy in alkali halides [3–5] and alkaline-earth halides [6]. The lanthanum halides have not been studied by transient induced absorption spectroscopy until the present work.

In $LaCl_3$, optically detected EPR of STEs [7] was found on both of the Cl-Cl pair axes that are directed out of the basal plane in the $LaCl_3$ crystal structure (the A and B sites in the terminology of Canning *et al.* [8]), and each was associated experimentally with one of the two identified STE luminescence bands [7]. The same study commented that the authors were unable to find a stable EPR signal of a V_k center in undoped or Ce-doped $LaCl_3$ after X irradiation at low temperature.

$LaBr_3$:Ce was discovered as a scintillator two years following $LaCl_3$:Ce [9]. It exhibits better light yield and gamma-ray energy resolution than $LaCl_3$:Ce, but many other aspects of their behavior as scintillators are similar. There has not yet been an ODEPR study of $LaBr_3$, so the findings of

*williams@wfu.edu

the Rogulis *et al.* study of $LaCl_3$ are often assumed likely to characterize $LaBr_3$ as well. Cerium-doped $LaBr_3$ is an important high-performance scintillator with applications in security inspection, medicine, and oil-well logging [10–12]. $LaBr_3$:Ce is one of the paradigms among scintillators in the sense that it was the first of a new generation of scintillator materials to dramatically exceed the energy resolution of the widely used alkali halide scintillator NaI:Tl as well as having a much faster pulse shape useful for timing applications and avoidance of pulse pile-up [9,13,14]. Furthermore, as bright and proportional as $LaBr_3$:Ce is, studies showed that it can be made even better by co-doping with divalent metal ions such as Sr^{2+} [14–16]. The physical mechanism for the latter finding is not yet fully understood. Fundamental time-resolved studies of excited states in $LaBr_3$ and $LaBr_3$:Ce as in the present work are helpful in understanding more fully how the material operates as a scintillator, and on that basis how it and related scintillators may be further improved by co-doping or other material engineering for specific applications.

An experimental study of $LaBr_3$:Ce luminescence and scintillation on nanosecond and longer time scales versus temperature and Ce concentration was conducted by Bizarri and Dorenbos [17]. The authors suggested a model in which prompt sequential capture of holes and electrons on Ce (labeled process I) was followed by slower thermally activated transfer of energy from diffusing STEs to Ce (processes II_{Fast} and II_{Slow}). The prompt capture was regarded as faster than 1 ns, since the luminescence of Ce^{3+*} excited ions with 16-ns radiative lifetime was the signal being measured. STE energy transport to Ce^{3+} was found to be thermally activated. Bizarri and Dorenbos measured STE luminescence as well as Ce^{3+*} luminescence, and deduced largely from the anticorrelation of their yields vs temperature that STE energy transport to Ce is more important than binary transport of self-trapped holes (V_k centers) and electrons. Other reasons for the conclusion are similar to those given in Ref. [18], including the absence of stable V_k centers in $LaCl_3$ and $LaCl_3$:Ce [7]. The optical transitions measured (absorption vs emission) of both STE and Ce excited states, and the measured time scales (0.5–700 ps versus 1 ns–4 μs) are different between the present study and that of Bizarri and Dorenbos. They are two important time windows on the same basic phenomena that contribute to recombination and scintillation in $LaBr_3$:Ce. The first steps to synthesize an understanding of the recombination physics from these complementary experimental perspectives are discussed in Conclusions. Rounding out the LaX_3:Ce family, LaI_3:Ce has been the subject of a few experimental and theoretical studies as well [19,20].

Picosecond measurements of excitation-induced absorption allow tracking energy transfer and evolution of trapped carriers and excited states faster than the 16-ns radiative lifetime of Ce^{3+*}. Modeling studies and previous picosecond absorption studies of alkali halide scintillators doped with Tl^+ have established that carrier trapping after hot-electron transport and the resulting establishment of electric fields governing subsequent transport in a particle track occur within a few picoseconds [21–23]. A challenge of undertaking picosecond absorption spectroscopy for the first time in a new material such as $LaBr_3$ is that one must first identify the transient absorption spectra of excited states of the host and of the activator. This study begins with that challenge.

II. EXPERIMENTAL METHOD

Samples for this study were grown, cut, polished, and encapsulated at Saint Gobain Crystals. Sample characteristics are summarized in Table I. Cerium dopant concentrations were measured by inductively coupled plasma atomic emission spectroscopy (ICP-AES). Partly because the not-intentionally doped ("undoped") sample was grown as a special scientific sample in a production furnace normally used for Ce-doped crystals, it had a trace Ce concentration measured as 0.0041 mole %. $LaBr_3$ samples doped with 4.4 mole% and 22 mole% Ce (measured by ICP-AES) completed the set of three samples studied in these experiments. For brevity, the figures and text references to follow will be labeled as "undoped $LaBr_3$," 4% Ce, and 20% Ce doped, referring to the same samples characterized more precisely above. The samples, of thickness 5 mm and diameter 12 mm, were processed in dry atmosphere before being sealed in cemented fused silica optical cells. Experiments in the present study were all conducted at room temperature, approximately 295 K.

The laser system comprises a Ti-sapphire oscillator and regenerative amplifier producing pulses at 840 nm with 200 fs pulse duration and about 3-mJ pulse energy at 10 Hz. Specifically, the system has a Coherent Verdi G7 diode driven continuous laser pumping a Coherent Mira 900 mode-locked oscillator whose output is amplified in a Positive Light regenerative cavity followed by a double-pass final power amplifier before recompression. The pulse is split to generate second harmonic (420 nm, 2.95 eV) and third harmonic (280 nm, 4.43 eV) pump pulses, which we can choose to bring to a soft focus in the sample to produce two-photon absorption across the band gap of $LaBr_3$ creating electron-hole pairs, or direct excitation of Ce dopant as described following. If the $LaBr_3$ is undoped, both of the pump wavelengths can reach the focus and produce interband excitation of the $LaBr_3$ host. However, if the sample is doped with 4% or 20% Ce, the 280-nm third harmonic photons are strongly absorbed by Ce^{3+} ($4f$-$5d$ transitions) as shown by the spectrum in Fig. 1.

As illustrated in the lower part of Fig. 2, before the third harmonic beam can come to a focus and produce two-photon interband excitation in a Ce-doped sample, it is absorbed and thus attenuated by direct excitation of Ce^{3+}. In contrast, the

TABLE I. Some properties of the $LaBr_3$ samples

Crystal	Ce in melt, mole%	Ce in crystal, mole%	pulse height, channel	resolution at 662 keV, %
$LaBr_3$ undoped	-	0.0041	No scintillation	N/A
$LaBr_3$:Ce (4%)	5.0	4.39	668	2.89
$LaBr_3$:Ce (20%)	20.0	22.21	828	5.58

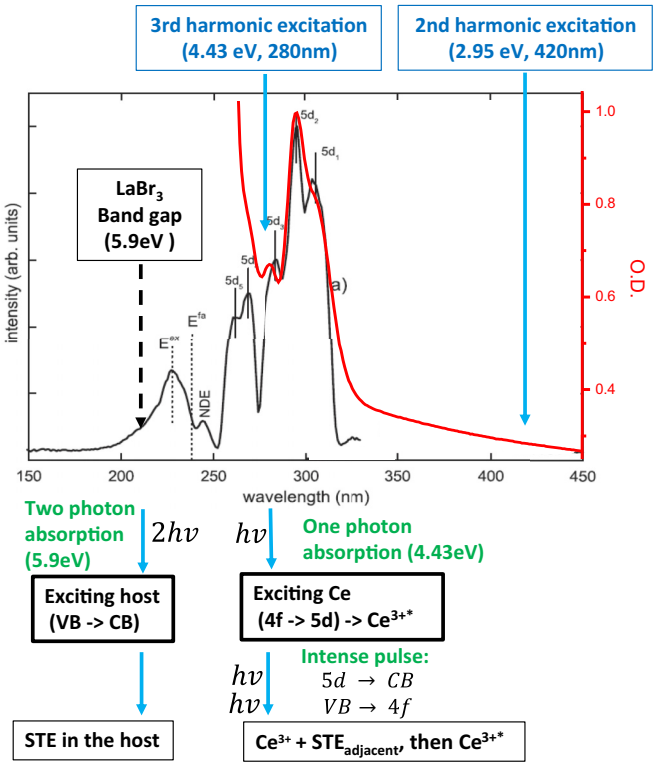

FIG. 1. The black line shows the excitation spectrum of Ce (5d-4f) luminescence at 10 K in $LaBr_3$:Ce reported by Dorenbos *et al.*, including their identification of Ce states and estimation of the exciton energy and band gap at 10 K [24]. The red line shows the spectrum of optical absorption at 295 K measured in our laboratory in the $LaBr_3$:Ce(4%) sample. The blue arrows show the photon energies of our second harmonic and third harmonic laser pulses in comparison to the spectrum of Ce^{3+} absorption.

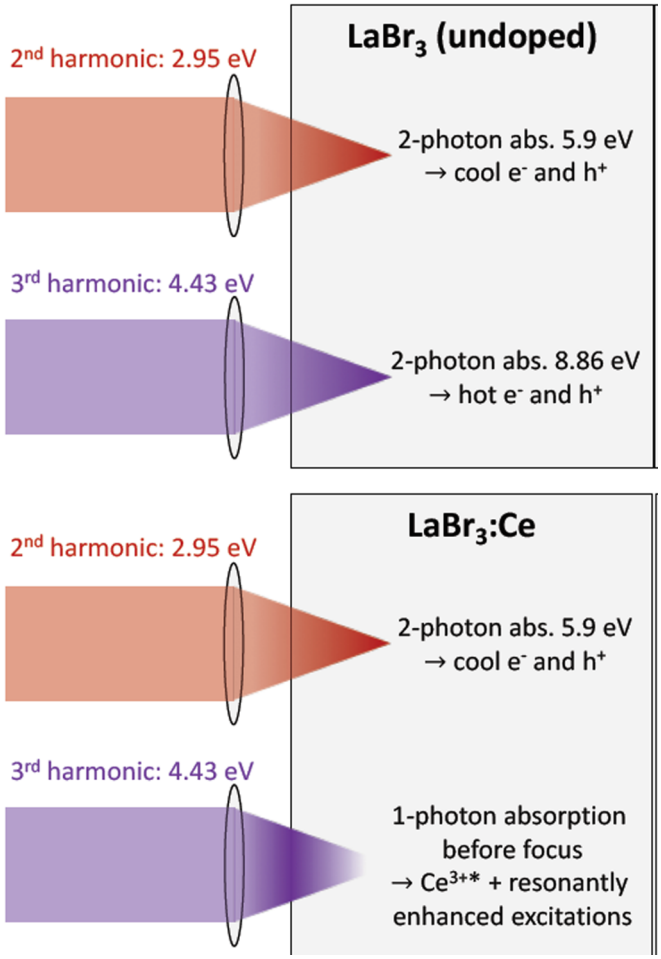

FIG. 2. Illustrations of different products and spatial distributions for excitation of undoped and Ce-doped $LaBr_3$ by the two laser harmonics used as pump pulses in this experiment.

second harmonic laser pulse at 420 nm lies below the Ce^{3+} absorption bands and will reach the focus at full power to produce two-photon host excitation even when Ce doping is present. Selecting the laser harmonic used for the pump pulse in Ce-doped samples thus controls whether the excitation is electron-hole pair generation in the host crystal of $LaBr_3$ and $LaBr_3$:Ce (comparable in some ways to scintillation conditions), or direct excitation of the Ce dopant itself. In the undoped samples, both laser harmonics produce mainly two-photon excitation of the $LaBr_3$. The free-carrier band gap of $LaBr_3$ at low temperature (10 K) has been estimated from luminescence excitation spectra as 5.9 eV, with an excitonic peak at 5.4 eV and empirical transparency gap of about 5.2 eV [24,25]. The free-carrier band gap of $LaBr_3$ at room temperature should be lower than the value at 10 K, perhaps 5.8 eV. Thus, two-photon absorption of the second harmonic pump pulse totaling 5.9 eV in our experiment produces free carriers near the band edges. In contrast, two-photon absorption of the 4.43-eV third harmonic in undoped $LaBr_3$ creates hot electrons and holes with the pair having excess energy of 3.06 eV above the band gap.

The probe pulses that assess the induced absorption are generated and detected in two ways depending on whether visible/ultraviolet or red/infrared spectral ranges are being measured. For visible/ultraviolet, a channel-plate intensified dual diode-array detector is used with a grating spectrograph as an optical multichannel analyzer (OMA) to capture the spectrum at a given pump-to-probe delay set by a mirror on a translation stage. A white-light continuum probe pulse is generated by focusing the fundamental or second-harmonic laser pulse in a sapphire plate. The dual diode array captures a reference spectrum directed around the sample on one array simultaneously with the transmitted spectrum on the other array to correct for pulse-to-pulse fluctuations in the continuum spectrum. In addition, each stored data spectrum at a given delay is the average of 100 laser shots. Measurements taken in this way exhibit noise fluctuations particularly along the time axis.

The channel-plate intensified OMA was not sensitive in the red and infrared spectrum, so an optical parametric amplifier (OPA) employing a beta barium borate crystal was tuned over the required infrared range, and its frequency-doubled output covered the red visible range. The OPA power per wavelength interval was much higher than that of the continuum, so measurement by a PbS detector sensitive from 1 to 2.9 μm and a biased Si photodiode for wavelengths below 1 μm was used. In this way, wavelengths from 575 to 3000 nm could be

measured with the OPA and doubled OPA output as the probe. At each delay setting, 30 shots were averaged. Time-delay data with this method were of good quality over the 0–200 ps range for each wavelength. Changing wavelength to acquire spectra required that the OPA be retuned for each wavelength, followed by pump/probe spot realignment as well. This was a source of possible noise from wavelength to wavelength in the spectra, and indeed there is a streakiness in the red/infrared spectra. Using both the continuum and OPA probe methods together, we could acquire induced-absorption data over a wide spectral range from 350 to 3000 nm or about 3.5 to 0.41 eV.

The excitation-induced change in optical density was calculated as described in Ref. [23]. Weak residual absorption due to defects created by interband excitation with the pump laser was produced at some ultraviolet and visible wavelengths. We are interested in transient induced absorption in the present study, so the residual absorption was subtracted. We tested whether luminescence was being detected in the transmission channel by blocking the probe and exciting with the pump pulse. If detected, the luminescence was subtracted from the transmitted signal spectrum before calculating induced absorption.

III. RESULTS AND DISCUSSION

A. Transient ultraviolet absorption spectra

The ultraviolet absorption was probed by a continuum pulse generated by the second harmonic laser pulse focused in a sapphire crystal and delayed relative to the pump pulse by a translation stage. Figure 3(a) shows a smoothed representation of the white light continuum (WLC) and the transmission curve of the filter chosen to prevent the 420 nm second harmonic pump pulse (also the WLC generating pulse) from entering the detection system. The V_k absorption band of KBr, taken as an example of alkali bromides, peaks at about 3.3 eV and has a full width at half maximum of about 0.6 eV at 10 K as shown in Fig. 5. Thus the necessary filter to block the laser second harmonic curtails measurements on the low-energy side of the likely range of V_k bands involving Br-Br ion pairs. Figure 3(b) illustrates that to block the 280-nm third harmonic pump pulse

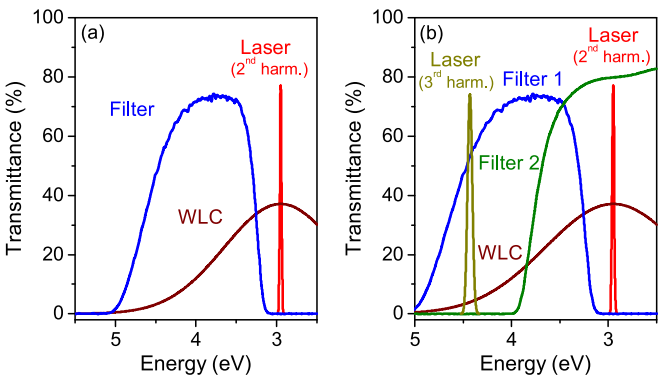

FIG. 3. Approximated spectrum of the white-light continuum (WLC) used for measurement, the laser pump spectral line, and transmission of the optical filter employed to block (a) the 2.95-eV laser line used both for pump and generator of WLC in second harmonic pumping, and (b) the 4.43-eV third harmonic pump and WLC generator.

and the 420-nm continuum generation pulse from entering the detector, a pair of filters transmitting photon energies only between 3.2 and 3.9 eV was used.

Figure 4 shows induced ultraviolet absorption spectra versus time (0–700 ps) for undoped $LaBr_3$ in the top row and 4% Ce-doped $LaBr_3$ in the bottom row. The contour plots in the left column display induced absorption (optical density) vs time increasing toward the reader, following excitation at $t = 0$ ps by the second harmonic 300-fs pulse, which produces two-photon host excitation in both undoped and Ce-doped $LaBr_3$. The persistent feature in both samples, lasting from a few picoseconds to at least 700 ps, is an absorption band centered near 3.3 eV and having a width of roughly 0.4 eV. The very strong peak at zero delay is believed to be due to two-photon absorption of a pump photon and a probe photon when they overlap temporally [26], not absorption by induced carriers, excitons, or defects. Unfortunately, this effect obscures the first picosecond of rising real absorption by the induced V_k centers or STE hole transitions. The data indicate that there may be a delay of about 10 ps between the pump-probe correlation peak and the rise to full O.D. of the suggested V_k or STE hole transition in $LaBr_3$. Canning *et al.* commented that their calculations indicated a barrier to V_k relaxation in $LaBr_3$ in the sense that they had to start the calculations from a distorted lattice with two bromines closer than equilibrium in order to initiate the V_k relaxation [8]. In alkali halides, a small barrier against self-trapping of excitons (11 to 33 meV in different alkali iodides) has been seen experimentally as free-exciton emission lines and delay of self-trapped exciton emission at low temperature [27,28], but no barrier against STH formation has been observed in alkali halides [5]. Deciding whether the present observations indicate a barrier to exciton self-trapping in $LaBr_3$ will require further experiments.

The central column of Fig. 4 shows the same data for second harmonic excitation plotted as a false-color two-dimensional map, with time increasing from top to bottom to match the time axis of the contour plots. Together, the left and center columns show in two plotting formats that two-photon excitation of electrons and holes in $LaBr_3$ with and without Ce doping produces broadband absorption near 3.3 eV. This is the same spectral region where Br_2^- V_k centers in KBr have their main absorption band [29]. We emphasize that this is the case in which electrons and holes are produced in the host lattice by two-photon interband excitation with the laser second harmonic.

The right-hand column of Fig. 4 shows ultraviolet absorption induced after third harmonic (280-nm) excitation. The 280-nm light does not produce two-photon excitation of the host crystal when Ce^{3+} is doped at substantial levels, but instead direct excitation of the Ce^{3+} dopant in a probable multiphoton cascade to be discussed later. The undoped $LaBr_3$ when excited by third harmonic does experience two-photon excitation at the focus, and exhibits a broad ultraviolet absorption band centered near 3.5 eV rather than 3.3 eV, but otherwise appearing similar to the absorption induced by the second harmonic.

In summary, the top row of Fig. 4 compares results for undoped $LaBr_3$ under two-photon excitation of the host producing carriers near the band edges from second harmonic (5.9-eV versus 5.8-eV band gap) in the center column, and

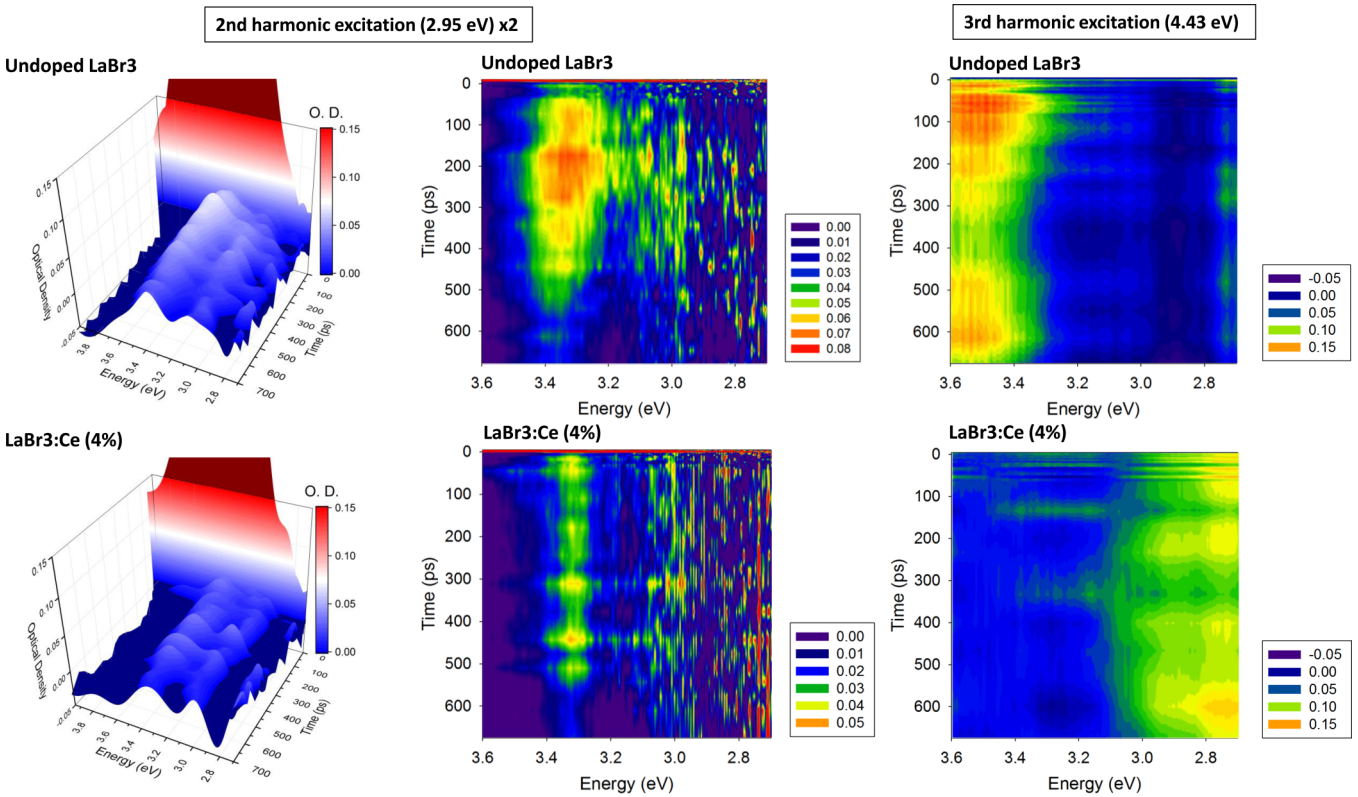

FIG. 4. Contour and color-map views of induced absorption in the ultraviolet spectral range where V_k-like absorption can be expected vs time after excitation. The top row shows results for undoped $LaBr_3$ and the lower row, 4% Ce-doped. The left and center columns are for second harmonic excitation which creates electron-hole pairs in the host $LaBr_3$ by two-photon absorption, while the right column is for third harmonic excitation which creates e-h pairs in the undoped $LaBr_3$ but excites Ce directly in $LaBr_3$:Ce(4%), rather than carriers in the host.

initially hot carriers from third harmonic excitation (8.86-eV versus 5.8-eV band gap) on the right. In both cases, an ultraviolet absorption band near 3.4 eV is produced. The bottom row of Fig. 4 makes a different comparison in the 4% Ce-doped sample: production of carriers near the band edges from second harmonic in the center lower figure versus direct excitation of Ce rather than production of carriers in the host $LaBr_3$ in the right lower figure. Notice that the right lower figure is missing the induced ultraviolet absorption band near 3.4 eV. This observation provides support for attributing the 3.3–3.5 eV absorption to a V_k-like transition. The 2.75-eV absorption in the lower right panel of Fig. 4 might be a charge transfer transition associated with excited Ce.

The transient spectra were averaged over the time interval from 5 to 500 ps and the result is plotted in Fig. 5. Superimposed on the time-resolved $LaBr_3$ and $LaBr_3$:Ce spectra in Fig. 5 is the published steady-state V_k spectrum in $KBr:NO_2$ at 77 K [29]. In alkali halides, the V_k spectrum has been found to be most strongly correlated with the halogen constituent, so the KBr V_k spectrum could be a reasonable guide to the peak energy and width that characterize Br-Br bonded pairs in another crystal such as $LaBr_3$. In the molecular orbital treatment by Jette, Gilbert, and Das [30], the ultraviolet V_k band was ascribed to a hole transition from the σ_u to the σ_g molecular orbital of the $(\text{halogen}_2)^-$ molecular ion.

The UV absorption band in Fig. 5 is probably not mainly produced by V_k centers (self-trapped holes) in $LaBr_3$. It is being observed in undoped $LaBr_3$ without known electron traps and in $LaBr_3$:Ce, where Ce^{3+} is unlikely to be an electron trap. It will be shown in the next section on infrared and visible absorption that self-trapped excitons, identified by their bound-electron transitions, are the dominant species produced within the first picosecond after excitation of $LaBr_3$. Therefore the

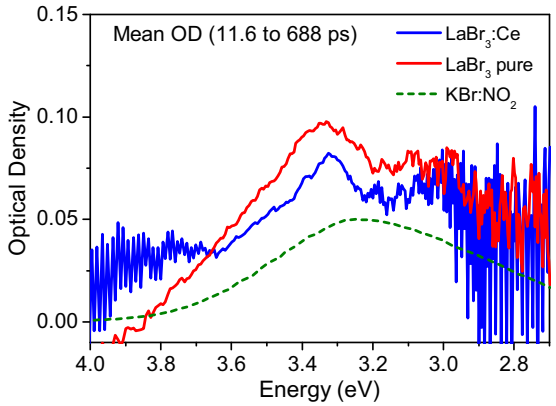

FIG. 5. The transient induced uv absorption spectra of $LaBr_3$ and $LaBr_3$:Ce(4%) were averaged over time from 12 to 690 ps. The probe light intensity becomes small (producing noise) below about 3 eV due to a filter (Fig. 3) and above about 4 eV due to poor continuum generation. The superimposed dashed line is the published steady-state V_k spectrum in $KBr:NO_2$ at 77 K [29].

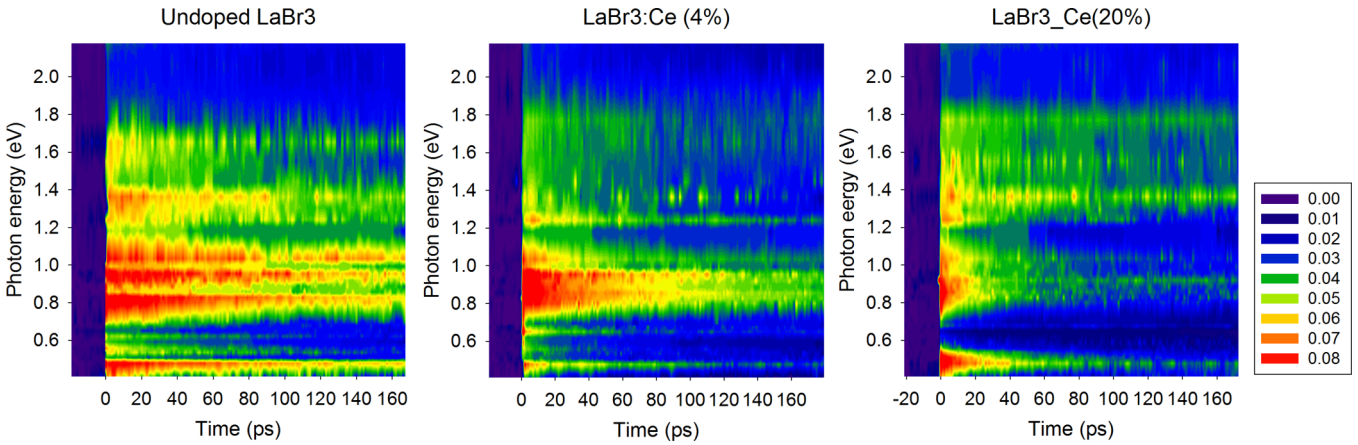

FIG. 6. Induced absorption (0–180 ps) of undoped (0.0041 mole% Ce), 4% Ce-, and 20% Ce-doped $LaBr_3$ after excitation by a 2.95 eV pulse of the laser second harmonic (two-photon excitation 5.9 eV). Zero on the time scale corresponds to pump/probe coincidence.

ultraviolet absorption band in Figs. 4 and 5 is attributed to the V_k-like hole transition of the STE in $LaBr_3$.

Calculations by A. Canning and M. del Ben, using hybrid density functional theory (PBE0), have found two theoretically stable STH configurations in $LaBr_3$, one associated with each of the out-of-plane halogen ion pair sites (denoted A and B) in the LaX_3 lattice [8]. The halogen pair in the basal plane (C) was not found to localize a hole or exciton in their calculations. The STH formed on the A and B sites was found theoretically to be "two-center" meaning there is a symmetrically relaxed $(Br_2)^-$ halogen molecular ion pair. The hybrid functional DFT calculations of V_k structure in $LaBr_3$ found Br-Br bond distance of 2.96 Å in the "site-A" V_k center and 2.89 Å in the "site B" V_k, referring to the two out-of-plane Br-Br configurations among the three that exist within the unit cell of $LaBr_3$ [8]. When a bound electron was added to the V_k core to form a STE, Canning *et al.* found that the V_k core on site A remained nearly on-center (V_k-like) in the STE, whereas the V_k core on site B was driven off-center in the STE [8], in the terms familiar from alkali halide STE relaxations [5,31].

B. Infrared absorption spectra: bound-electron transitions of STE and effects of Ce doping

Having looked in the ultraviolet spectral range at the $\sigma_u \rightarrow \sigma_g$ hole transition between molecular orbitals of the diatomic halogen core of the STE, we now present induced picosecond absorption spectra in the infrared and red-visible ranges in Figs. 6 and 7. Interpretation of the spectra will take into account what has previously been learned about STE relaxation and transitions of the bound outer electron in alkali halides. When a self-trapped hole in alkali halides captures an electron in a bound excited state, the halogen molecular-ion pair on which the STH resides may translate off-center with respect to the normal V_k configuration [5,31–33]. Configurations of increasing translational relaxation of the pair's midpoint vary in alkali halides from zero (called type I or "on-center"), to intermediate (type II or "weakly off-center"), where the trailing halogen of the pair has not fully cleared its cation cage, to type III or "strongly off-center," where the trailing halogen of the pair has cleared the cation cage creating a relaxed electronic excited state resembling a nearest-neighbor defect pair of an electron-occupied vacancy (nascent F center) and a nearest-

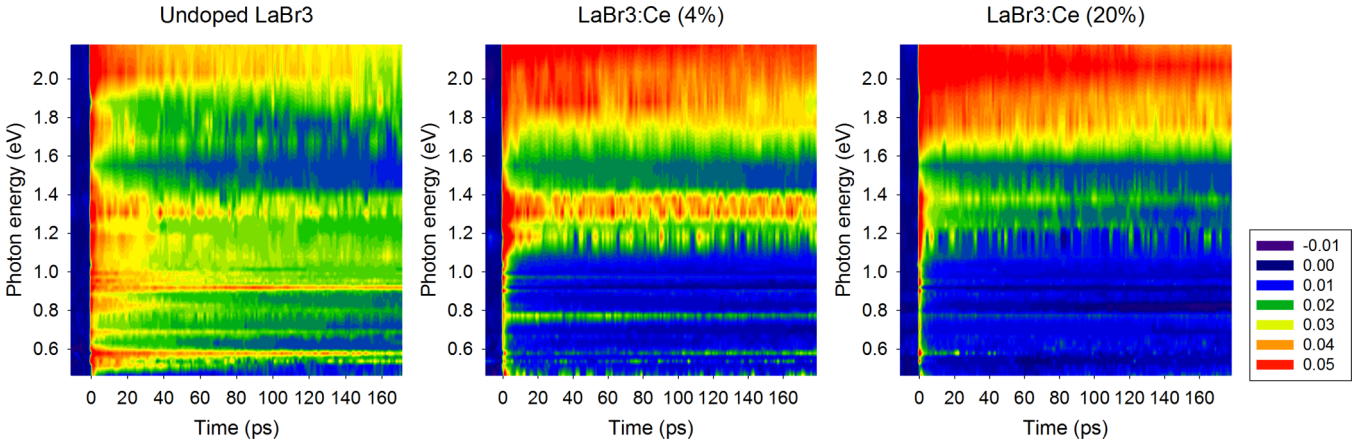

FIG. 7. Excitation-induced absorption (0–180 ps) of undoped (0.0041 mole% Ce), 4% Ce-, and 20% Ce-doped $LaBr_3$ after excitation by a 4.43-eV pulse of the laser third harmonic, which produces two-photon 8.86-eV excitation of the undoped sample or direct excitation of Ce in doped samples.

neighbor interstitial halogen molecular ion [5,32]. Which configurations occur in a given alkali halide is determined mainly by ion-size factors and energy minimization as the STE outer electron wave function is progressively able to approach that of an F center electron [5].

Previously studied self-trapped exciton absorption spectra in alkali halides have shown that when the off-center relaxation of the halogen molecular-ion core of the STE is small to moderate, the excited state absorption transitions of the outer bound electron component of the STE tend to be in the infrared spectral range [5]. This makes sense at a conceptual level because in the absence of large lattice relaxation, the outer electron may be considered bound mainly by Coulomb attraction to the self-trapped hole. Regarding the attractive potential simply as the screened charge of a localized hole, the binding energy of the electron in the on-center STE could be expected to be similar to its binding energy in a free exciton, which is a few tenths of an eV in halide insulators, depending on the dielectric constant. The STE in NaI occurs only as type I (on-center halogen ion pair), and exhibits its bound electron transitions at ∼0.2 eV [34]. CsI exhibits STEs with both types I and II (mildly off-center) lattice relaxation [27,35]. From the 5.9-eV free-carrier band gap and 5.4-eV exciton absorption peak in $LaBr_3$ estimated from synchrotron excitation experiments at $T \approx 10$ K by Dorenbos *et al.* [24], one may deduce a free-exciton binding energy in $LaBr_3$ of about 0.5 eV. Based on this, we should look for an on-center STE in $LaBr_3$ to have ∼0.5-eV binding energy.

As the STE relaxes off-center, the halogen diatomic core moves to open up a partially formed halogen vacancy in the space left behind. The binding energy of an electron in a fully formed halogen vacancy is that of an F center, known to be 1 to 2 eV depending on the alkali halide. The electron binding energy in type II and III STEs approach toward the F center binding energy in that material to the degree that the STE resembles an F center still partially occupied by a halogen molecular ion pair or an F center with a neighboring interstitial molecular ion pair (H center), respectively. Such a partial or full vacancy can accommodate the bound excited electron of the STE in a lower energy configuration than the on-center STE binding energy estimated above as 0.5 eV or less. Based on type-III STE absorption peaks near 1.5 eV in the alkali bromides KBr and RbBr [3,5] we might look for type-III STE absorption bands in $LaBr_3$ at a similar energy and type-II bands intermediate between types I and III at around 1 eV.

Figures 6 and 7 display induced absorption spectra from 570 to 3000 nm on the 0–180 ps scale, for host excitation (second harmonic) and direct Ce excitation if doped (third harmonic), respectively. Figures 8 and 9 present corresponding data measured on a finer time scale from 0–14 ps.

Consider first the results of $LaBr_3$ host excitation in Fig. 6. Our initial interest is in the spectrum without focusing on the time dependence. In the rightmost figure for $LaBr_3$:Ce(20%), a division of the induced absorption spectrum into three parts can be most clearly seen. There is an intense band at the lowest energy measured, with a peak evidently at about 0.47 eV. Then there is a fully observed broad band or group of narrow bands extending from 0.7 to 1.15 eV. Finally, from 1.2 to 1.8 eV, there is a third grouping of absorption bands, more broadly dispersed than the other two groupings. We noted in the Experimental Method section that retuning the OPA for each wavelength could lend streakiness to the spectra within each identified grouping. On the other hand, Canning and del Ben point out that there are three different Br-Br pair environments in the unit cell of $LaBr_3$ [8], so there is a possibility of multiple STE sites with different transition energies comprising each group. Until these possibilities are resolved, we will discuss the absorption in terms of the three evident large groupings rather than individual bands on the finer scale.

Looking back toward the left in Figs. 6 and 8 at the color maps of induced absorption in $LaBr_3$:Ce(4%) and undoped $LaBr_3$, it will be seen that the same three spectral groupings can be recognized as were noted in the 20% Ce sample. The bands decay more slowly as the amount of Ce doping decreases. A strong but narrow 0.47-eV band is seen in the undoped and Ce-doped samples at the bottom of our spectral range.

In line with the alkali halide examples cited in the opening paragraph of this section, as well as additional evidence on the effect of third harmonic excitation to follow, we tentatively identify the band near 0.5 eV as the outer electron excitation of

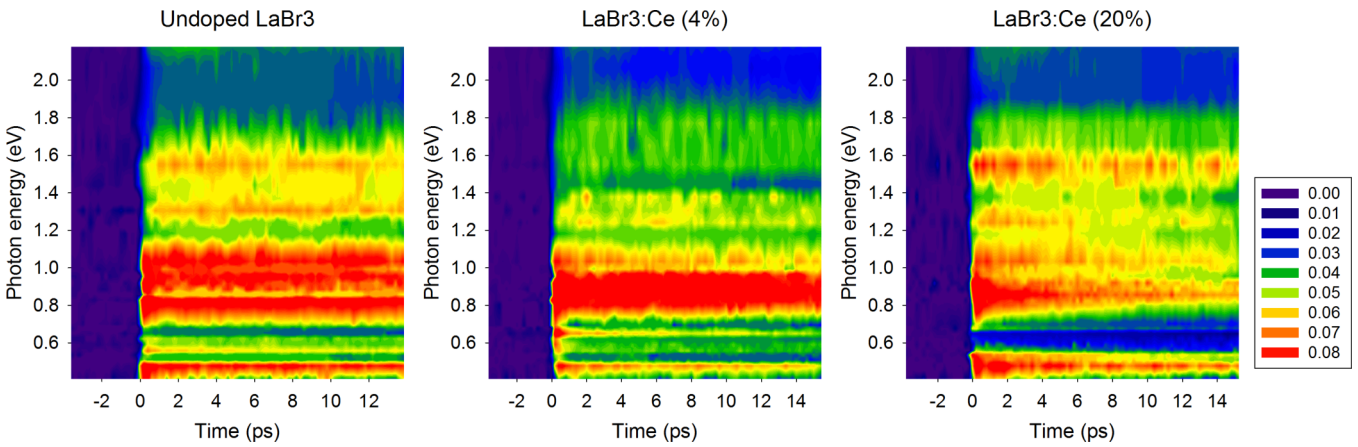

FIG. 8. Excitation-induced absorption (0–14 ps) of undoped (0.0041 mole% Ce), 4% Ce-, and 20% Ce-doped $LaBr_3$ after excitation by a 2.95-eV light pulse (two-photon energy 5.9 eV). Zero on the time scale corresponds to pump/probe coincidence. These are repeated measurements as in Fig. 6 taken with finer time resolution.

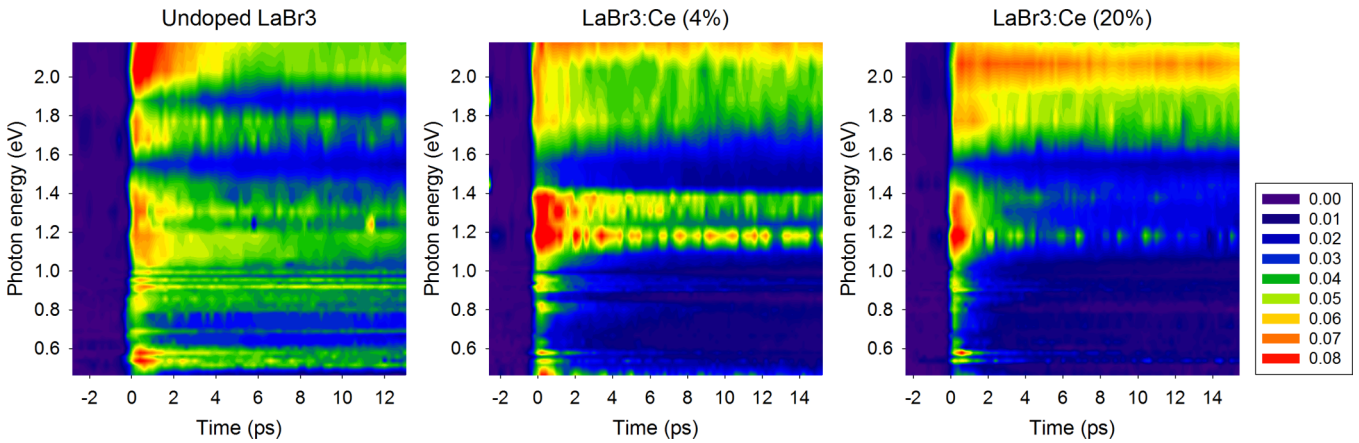

FIG. 9. Excitation-induced absorption (0–14 ps) of undoped (0.0041 mole% Ce), 4% Ce-, and 20% Ce-doped $LaBr_3$ after excitation by a 4.43-eV light pulse (two-photon energy 8.83 eV).

the on-center (type I) STE in $LaBr_3$ with or without Ce doping. The completely observed band or grouping in the middle range from 0.7 to 1.2 eV in Figs. 6 and 8 is likewise attributed to outer electron excitations of a weakly off-center (type II) STE. Finally, the broad band or grouping from 1.25 to 1.8 eV in Figs. 6 and 8 is attributed to strongly off-center (type III) STEs.

Figure 7 displays spectra of the same three samples, this time with excitation by third harmonic laser pump pulses at 4.43 eV. Comparing to Fig. 6, there are at least two dramatic changes in the induced absorption spectra of Ce-doped samples when excited directly in the Ce^{3+} absorption band. The lower half of the false-color map goes blue, indicating little induced absorption in the infrared STE bound-electron region in the Ce doped samples. At the same time, the upper 1/3 of the photon energy range goes red, indicating intense absorption. This same region was mostly blue in Fig. 6. As discussed in the Experimental Methods section and Fig. 1, we expect that the third harmonic pump pulse in Ce-doped samples is absorbed mainly in direct excitation of the Ce^{3+} $4f$-$5d$ transition, suppressing the intensity at the focus, which could excite free carriers by two-photon interband transitions. Hence absorption features that are strong with second harmonic excitation (Figs. 6 and 8) and suppressed with third harmonic excitation (Figs. 7 and 9) can be interpreted as resulting from creation of electrons and holes in the host crystal itself. The bands suppressed in Figs. 7 and 9 clearly include the ones identified as type-I and type-II STE electron transitions. We regard this dependence on excitation wavelength as confirmation of the STE assignments. The suggested type-III band(s) have a less clear behavior, but are in any case changed under third harmonic excitation.

Figures 8 and 9 are not simply expanded plots of the same data as Figs. 6 and 7, but separate measurements taken at finer spacings on the optical delay stage. The main bands rise to their initial maximum in less than 1 ps. In undoped $LaBr_3$ with second harmonic excitation, the bands remain basically unchanged over the duration of the 14-ps range in Fig. 8, and almost so for the 4% Ce-doped sample.

The appearance of a strong new band in the 2.0 to 2.2 eV range after direct excitation of Ce^{3+} in the Ce-doped samples by the laser third harmonic in Figs. 7 and 9 implies that the 2.1 eV band is a signature of excited or ionized Ce^{3+} ions. Charge transfer transitions involving the ionized charge state Ce^{4+} or the excited state Ce^{3+*} (responsible for Ce luminescence and scintillation) are the main possibilities to be considered. The left diagram of Fig. 10 shows the energy of the ground state of the Ce^{3+} ion in $LaBr_3$ calculated by Dorenbos [36] to be 0.5 eV above the valence-band maximum (VBM) using the chemical shift model [37] together with values of the inter-$4f$-electron Coulomb repulsion energy and the $5d$-centroid shift determined from spectroscopy as described in [36]. An earlier estimate of 0.9 eV $\pm$ 0.4 eV for the Ce^{3+} VBM energy [24] is in agreement within its uncertainty. The Ce^{3+} ground state would be the lattice-relaxed final state of a charge-transfer (CT) transition of a valence electron into Ce^{4+}. In Ref. [38], Dorenbos presented evidence for an empirical rule that the onset of CT transitions from the valence band to Ce^{4+} corresponds approximately to the energy of the Ce^{3+} ground state with respect to the VBM. It was pointed out that the width of the VB $\rightarrow$ Ce^{4+} CT band is typically large. Blahuta *et al.* measured the VB $\rightarrow$ Ce^{4+} CT band in LYSO:Ce:Mg annealed in an oxidizing atmosphere and it extends about 1 eV from onset to the maximum of absorption [39]. If the band width is similar in $LaBr_3$:Ce, we might expect the onset of VB $\rightarrow$ Ce^{4+} CT absorption to be about 0.5 eV with a broad peak near 1.5 eV in $LaBr_3$:Ce. This is indicated schematically in the middle panel of Fig. 10. The Gaussian band is meant to suggest an optical absorption spectrum rising up from 0.5 eV to a peak near 1.5 eV, but not to imply that there is such a distribution of final states in the band gap. The broad width of the optical band might reflect a broad density of initial states in the valence band.

Experimentally, in Figs. 7 and 9, we do not find evidence of induced absorption at 1.5 eV or below that clearly increases in proportion to the Ce doping. The strong induced absorption band that increases with Ce doping is at 2.0 to 2.2 eV, higher in energy than seems likely for the Ce^{4+} absorption peak. We suggest a different attribution for it below. In Fig. 9, there appears to be a weak Ce dependence of absorption near 1.75 eV. This signal and its Ce-dependence is weak compared to the 2.0–2.2 eV absorption, so if the 1.75-eV band is attributed to VB $\rightarrow$ Ce^{4+} CT absorption, the number of Ce^{4+} charge states produced even by direct (high intensity) laser excitation of Ce

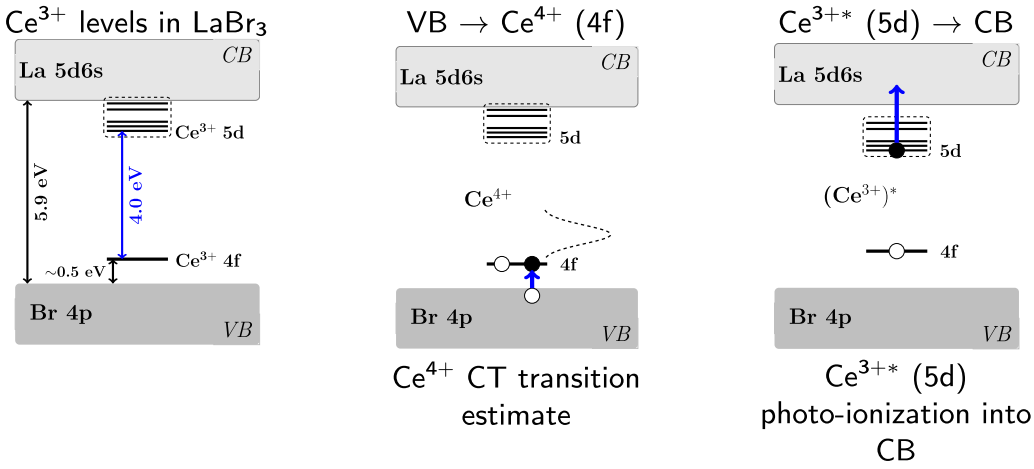

FIG. 10. Schematic energy levels involved in (a) $4f$-$5d$ excitation of Ce^{3+} and [(b) and (c)] two possible charge transfer transitions that might account for the strong 2.1-eV absorption band induced by direct excitation of Ce in Fig. 7. We suggest that photoionization of Ce^{3+*} to the conduction band is the most likely identification.

appears to be much smaller than whatever is causing the 2.1-eV absorption after direct laser excitation of Ce.

For reasons described in the following, we suggest that the 2.0–2.2 eV absorption band seen in Fig. 7 after exciting Ce^{3+} is the photoionization of the $5d$ electron from the Ce^{3+*} excited state into the conduction band as illustrated on the right side of Fig. 10. The challenge to consider is whether the 2.1-eV transition energy fits along with other energy steps and transitions that promote an electron from the top of the valence band to final states in the conduction band, given the 5.9-eV band gap of $LaBr_3$. Consider the following sequence of transitions and energy steps as depicted in Fig. 11: (a) energy of $Ce^{3+}(4f)_{\text{relaxed}}$ with respect to VBM ≈ 0.5 eV [36]; (b) optical absorption

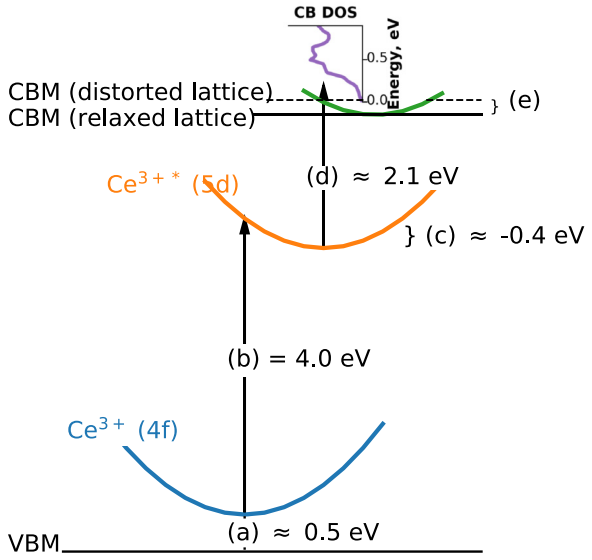

FIG. 11. Energy intervals, transitions, and lattice relaxations promoting an electron from the valence band top through ground and excited states of Ce^{3+} and Ce^{3+*}, respectively, terminating in the conduction band with density of states calculated by Aberg *et al.* [40].

$Ce^{3+}(4f)_{\text{relaxed}} \rightarrow Ce^{3+*}(5d)_{\text{unrelaxed}} = 4.0$ eV [24]; (c) lattice relaxation $Ce^{3+*}(5d)_{\text{unrelaxed}} \rightarrow Ce^{3+*}(5d)_{\text{relaxed}} \approx -0.4$ eV $\approx {}^1/_2$ Stokes shift Ce^{3+*} ($5d$-$4f$); (d) optical absorption $Ce^{3+*}(5d)_{\text{relaxed}} \rightarrow$ electron in CB + $Ce^{4+}_{\text{unrelaxed}} \approx 2.1$ eV (this work); (e) lattice distortion in optical final state $Ce^{4+}_{\text{relaxed}} \rightarrow Ce^{4+}_{\text{unrelaxed}} \approx 0.X$ eV; and (f) peak of final electron DOS relative to CBM ≈ 0.5 eV if corresponding to CB DOS [40].

Starting from the valence band maximum (VBM), the energy of $Ce^{3+}(4f)_{\text{relaxed}}$ has been calculated to be 0.5 eV as noted above [36]. It was measured by XPS in the closely related material $CeBr_3$ as 1.0 eV ± 0.8 eV [41]. The measured optical absorption transition from $Ce^{3+}(4f)_{\text{relaxed}}$ to $Ce^{3+*}(5d)_{\text{unrelaxed}}$ is 4.0 eV at 10K [24]. The configuration coordinate lattice relaxation from $Ce^{3+*}(5d)_{\text{unrelaxed}}$ to $Ce^{3+*}(5d)_{\text{relaxed}}$ is estimated as −0.4 eV, taken as half of the Stokes shift of Ce^{3+*}($5d$-$4f$) luminescence in $LaBr_3$. This step is added with a negative sign because it is a step downward in progress across the gap. The optical absorption transition from $Ce^{3+*}(5d)_{\text{relaxed}}$ to a final photoionized state of an electron in the conduction band + $Ce^{4+}_{\text{unrelaxed}}$ is assigned our experimentally observed value of 2.1 eV, which is the hypothesis being tested.

The sum of the steps (a)–(d) is 6.2 eV, which exceeds the 5.9-eV (low-temperature) band gap of $LaBr_3$ by 0.3 eV. This is a minor disagreement if the peak of the 2.1-eV absorption band is regarded as coinciding with the conduction band minimum (CBM) of $LaBr_3$ with a perfect lattice. Aberg *et al.* have calculated the conduction band density of states (DOS) of $LaBr_3$ [40] and also confirmed that the joint density of states matches at least the first 3 eV of measured interband absorption [41]. Their CB DOS for the first 0.9 eV above the CBM is reproduced in the top of Fig. 11 to represent our suggestion that the 2.1-eV absorption band final state should correspond roughly to the first significant peak in the CB DOS, which is about 0.5 eV above the CBM. The band structure of $LaBr_3$ is somewhat unusual in the slow rise of DOS from the CBM onset to the first significant peak, in common with the lower conduction band structure of another very good scintillator SrI_2 as previously noted by Setyawan *et al.* [42]. Finally, the conduction band state populated by the

photoionization transition is in a lattice distorted according to the relaxed configuration of the $Ce^{3+*}(5d)_{relaxed}$ state that was photoionized. This unknown but probably small addition to the band gap energy should raise the conduction band by $0.X$ eV, where $0.X$ may be of order 0.3 eV. In summary, the sequence of energy steps in Fig. 11 and the list as discussed appears consistent with our assignment of the 2.1-eV photoionization transition.

Further support for the conclusion of Fig. 11 is available directly from the calculated Ce^{3+} ($5d$) electron binding energy of about 1.3 eV below the conduction-band minimum (CBM) of $LaBr_3$ given in Ref. [36]. With respect to Fig. 11 starting from relaxed Ce^{3+*} ($5d$), we may add 1.3 eV + [$0.X = 0.3$ eV in step (e)] + (0.5 eV to the peak of the CB DOS) to obtain 2.1 eV for step (d) in Fig. 11. The two routes are consistent, and in these terms a 2.1-eV absorption band peak for ionization of Ce^{3+*} ($5d$) excited ions seems reasonable.

Looking again at Figs. 7 and 9, the undoped sample does not suffer suppression of the absorption bands in its lower half spectral range when excited with 280-nm pulses, in contrast to the Ce-doped samples. This is reasonable because there is not a significant concentration of Ce in the undoped sample to deplete the third harmonic pump light. The (almost) full-strength pump pulse thus reaches its focus and produces interband excitation of the host, this time ending in hot carriers (8.86-eV excitation energy versus 5.8-eV band gap). The end result of third harmonic excitation in the undoped sample is creation of similar infrared absorption bands that we have already attributed to STE electron transitions. Recall the similar behavior versus Ce doping and laser harmonic observed in ultraviolet spectroscopy of the STE hole transition in Fig. 4. On the other hand, a 2.1-eV band is also found (being attributed to excited Ce^{3+*}) in the undoped sample produced by third harmonic excitation. The undoped sample contains 0.0041 mole% Ce. This is apparently enough to produce some 2.1-eV absorption when directly excited, but not enough to prevent or significantly suppress two-photon interband excitation of the $LaBr_3$ host.

Figure 9 shows data for the same samples and 0–14 ps time range as Fig. 8, but for a third harmonic (4.43-eV) pump pulse producing direct excitation of the Ce^{3+} dopant in the 4% and 20% Ce samples. In the undoped sample, the absorption bands at about 0.55 eV, about 0.9 eV, and about 1.25 eV attributed to types I, II, and III STE are seen similar to Fig. 8, except instead of rising to full intensity and remaining there for most of 14 ps, the bands now have a component that is produced quickly but decays with a characteristic time of about 1 ps. For reasons to be discussed below, we attribute the rapidly decaying component of the STE bands under third harmonic excitation to the special location of STEs created immediately adjacent to Ce^{3+} substitutional ions by three-step excitation of Ce^{3+}. Within this hypothesis, illustrated in Fig. 12, the rapid 1-ps decay indicates conversion of the adjacent STE to the excited state of Ce^{3+}, i.e., Ce^{3+*}. Specifically, this 1-ps lifetime will be attributed to the dipole-dipole transfer time from STEs directly adjacent to the Ce^{3+} ion. In the highly-doped 4% and 20% samples, we see in Fig. 9 a dominance of the rapidly decaying component of the attributed types I and II STE bands, indicating that most of the pump photons are expended exciting Ce directly in these crystals to produce adjacent STEs as proposed below.

The high-intensity excitation of Ce^{3+} ions probably produces the first excitation within Ce^{3+} itself as a $4f$-$5d$ transition. Since the amplified fs pulse is at high intensity, we can expect that there will be a high number of second and third excitations of the excited Ce^{3+*} real intermediate state. The second excitation of what is now Ce^{3+*} could put the Ce $5d$ electron into the conduction band, leaving Ce^{4+} and a conduction electron nearby. A third excitation by the intense laser pulse could fill the Ce $4f$ hole by charge transfer from the valence band. One result of intense excitation of a Ce^{3+} ion could thus be creation of an electron-hole pair initially on the shell of host $LaBr_3$ ions adjacent to the Ce^{3+} ion at which the resonantly enhanced multiphoton transition occurs. This is what we suggest is the origin of the very early and short-lived (~1 ps) STE-like absorption spectrum in Ce-doped samples that are excited by 4.43-eV photons, illustrated in Fig. 12. The decay time of STE absorption in ~1 ps could then represent the time for dipole-dipole transfer of the STE energy to Ce^{3+} at the closest separation. Under these excitation conditions in the Ce-doped $LaBr_3$ samples, the 2.1-eV absorption attributed to Ce^{3+*} is formed within ~1 ps.

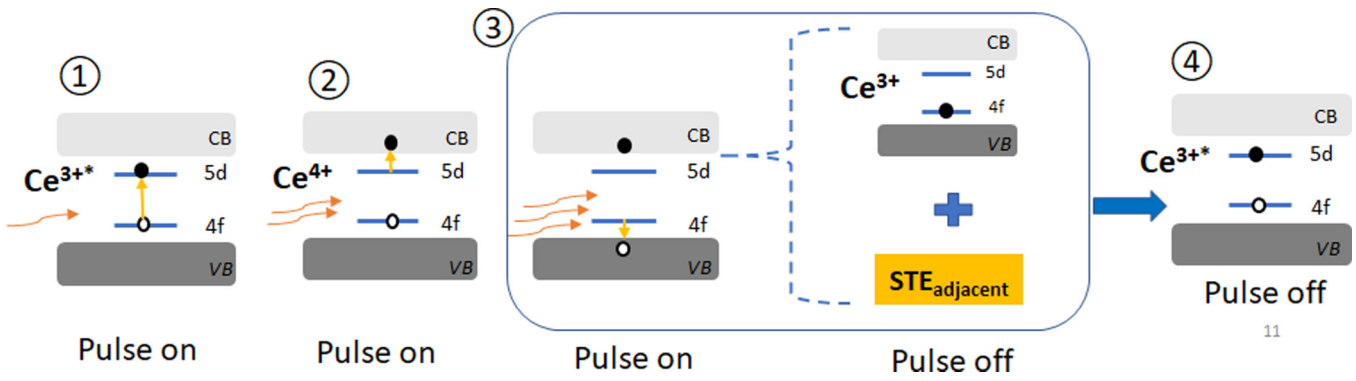

FIG. 12. Possible steps in high-intensity femtosecond excitation of a Ce^{3+} dopant ion by the third harmonic laser pulse, exciting $4f$-$5d$ transitions directly. Three sequential excitations including charge transfer (pulse on) could leave Ce^{3+} in its electronic ground state with an electron and a hole transferred to the shell of adjacent ions. The (pulse off) schematics illustrate that the transferred electron and hole could form an STE on the nearest-neighbor ion shell adjacent to Ce^{3+}, which could be followed by dipole-dipole energy transfer from that closest site.

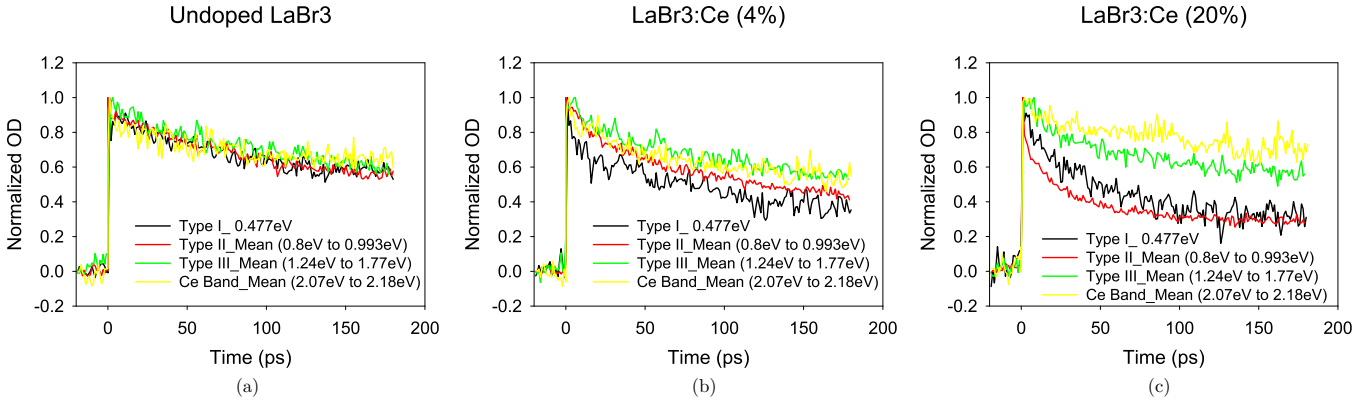

FIG. 13. [(a)–(c)] Induced absorption normalized at its initial peak is plotted vs time for types I, II, and III STE bands and for the spectral region of 2.1 to 2.2 eV in which an absorption band of Ce^{3+*} is believed to occur. All of these decay data were measured following second harmonic pulse excitation which creates electrons and holes throughout the $LaBr_3$ host lattice. The time-dependent absorption has been averaged over spectral ranges associated with each band as follows: STE I = 0.47 eV; STE II = 0.8 to 0.993 eV; STE III = 1.24 to 1.77 eV; Ce^{3+*} = 2.07 to 2.18 eV.

C. STE decay rates

It can be seen on inspection that the decay times of the absorption bands in Fig. 6, which we attribute to type-II STE (0.7–1.1 eV) and type-I STE (upper edge visible at 0.46 eV), become shorter as the Ce concentration increases from 0.0041% to 4%, to 20%. The absorption bands from 1.25 to 1.8 eV attributed to type-III STE have a similar but less obvious decay-time dependence on Ce concentration. Additionally, the excited Ce absorption band is found in the range 2.0 to 2.2 eV. The decay curves for all four of these spectral regions in samples with the three Ce concentrations are plotted as a compact survey comparison in Figs. 13(a)–13(c). The complete set of data were fitted to a single exponential decay plus a constant, for each band type and Ce concentration. Figure 14 shows preliminary induced absorption data out to 5 ns. The fitted plots are shown in Figs. 15–18. Values of the decay time, pre-exponential coefficient, and constant are tabulated for the 12 curves in Table II.

The following generalizations can be made. In Fig. 13(a) for the undoped sample with host excitation (second harmonic), the decay curves of all three STE types and the spectral range of the "Ce* band" are almost identical in the 0–180 ps range. For the three STE types, it is not unexpected to find similar decay rates. On the other hand, a Ce^* band produced as a result of energy transfer from STE should grow as the STE decays. Finding nearly the same decay characteristics at the Ce^* band wavelength near 2.1 eV could occur if there is a background of STE absorption underlying that spectral range.

Figures 8 and 13, measured following 5.9-eV excitation of the $LaBr_3$ host show that self-trapped excitons in $LaBr_3$ and $LaBr_3$:Ce are formed at their maximum population within less than 1 ps of (cool) e-h pair generation. Figure 9 shows that excitation of hot e-h pairs (total energy 8.86 eV) in undoped $LaBr_3$ also creates STEs at their maximum population within 1 ps. This is worth noting because scintillation should resemble the case of hot e-h pair production.

The data summarized in Table II demonstrate that roughly 50% of the created STEs decay with time constants of tens of picoseconds. The decay is faster and the fast-decaying fraction is larger for higher Ce concentration. Averaging the tabulated data for the types I, II, and III STE bands, the STE decay time is about 92, 69, and 38 ps respectively in undoped, 4% Ce-, and 20% Ce-doped $LaBr_3$. In the same sequence, the averaged values of the coefficients A of the exponentially decaying STE bands are 0.033, 0.035, and 0.044 in undoped, 4% Ce-, and 20% Ce-doped $LaBr_3$. After this fast decay stage occurring in tens of picoseconds in Ce-doped samples, roughly 50% of the absorption remains. The fraction remaining depends on Ce concentration and is fitted as a constant, B, in the 0–180 ps range of the present data. We expect that it is not a constant, but the coefficient of a later stage or stages of STE decay occurring in the nanoseconds time range in these room-temperature measurements.

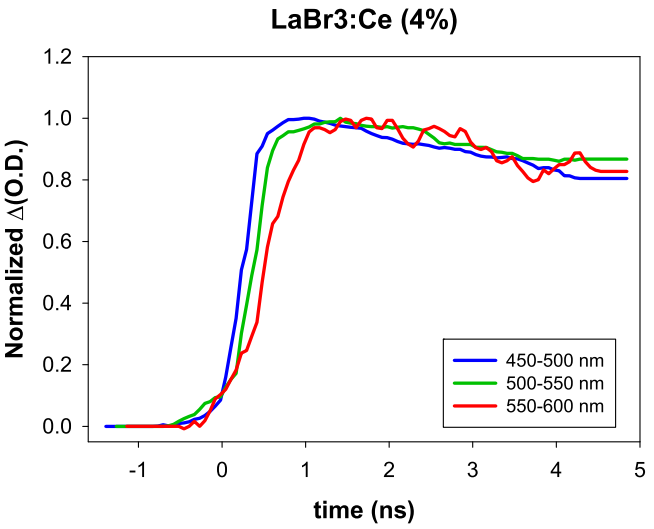

FIG. 14. Induced absorption measured on a nanosecond time scale. The sample is excited by 300-fs laser pulses producing 5.9-eV host excitation as in other parts of this work, but the induced absorption is measured with a xenon flashlamp and streak camera. Trigger jitter of the streak camera, averaged over many measurements produces a slowing of the rise time. Comparing the indicated wavelength ranges suggests that the 550–600 nm (average 2.15 eV) absorption rise is slower than the jitter contribution.

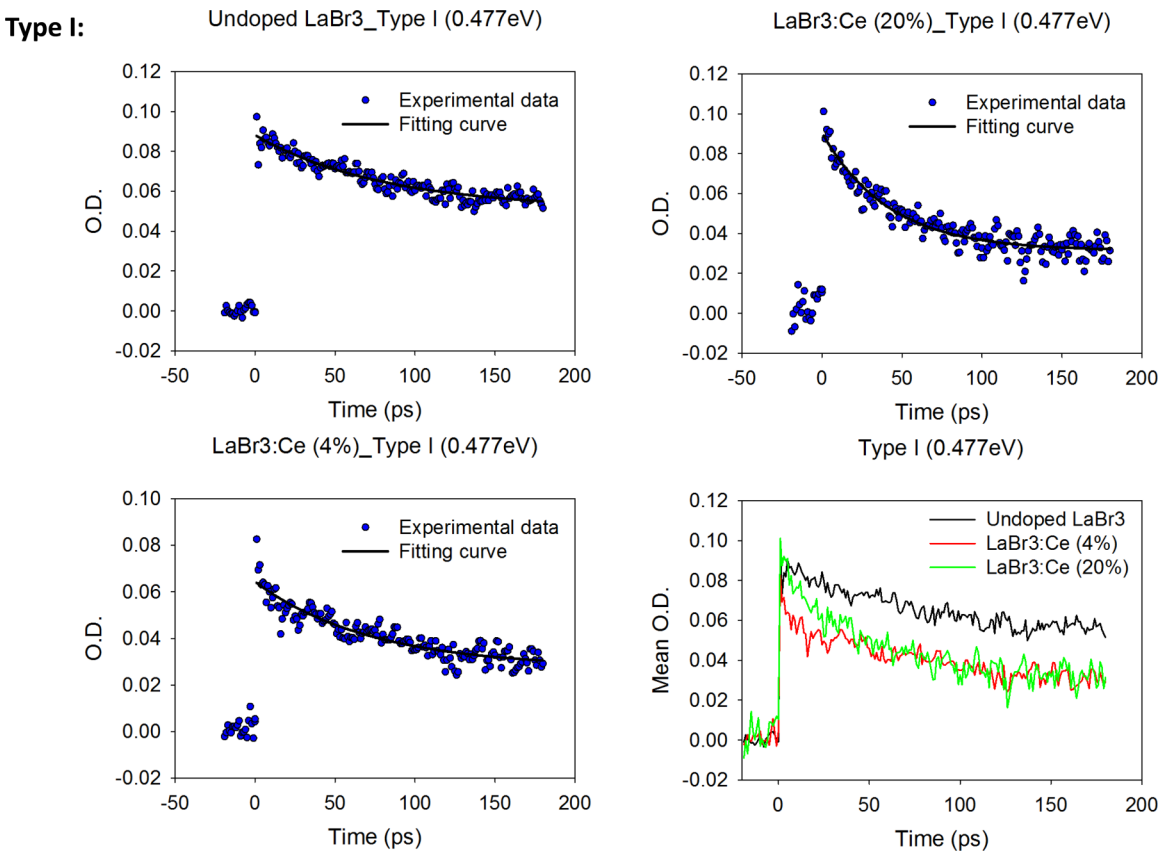

FIG. 15. Absorption at the wavelength range of type I STEs induced by second harmonic excitation is shown fitted by a single exponential decay and a constant, listed in Table II.

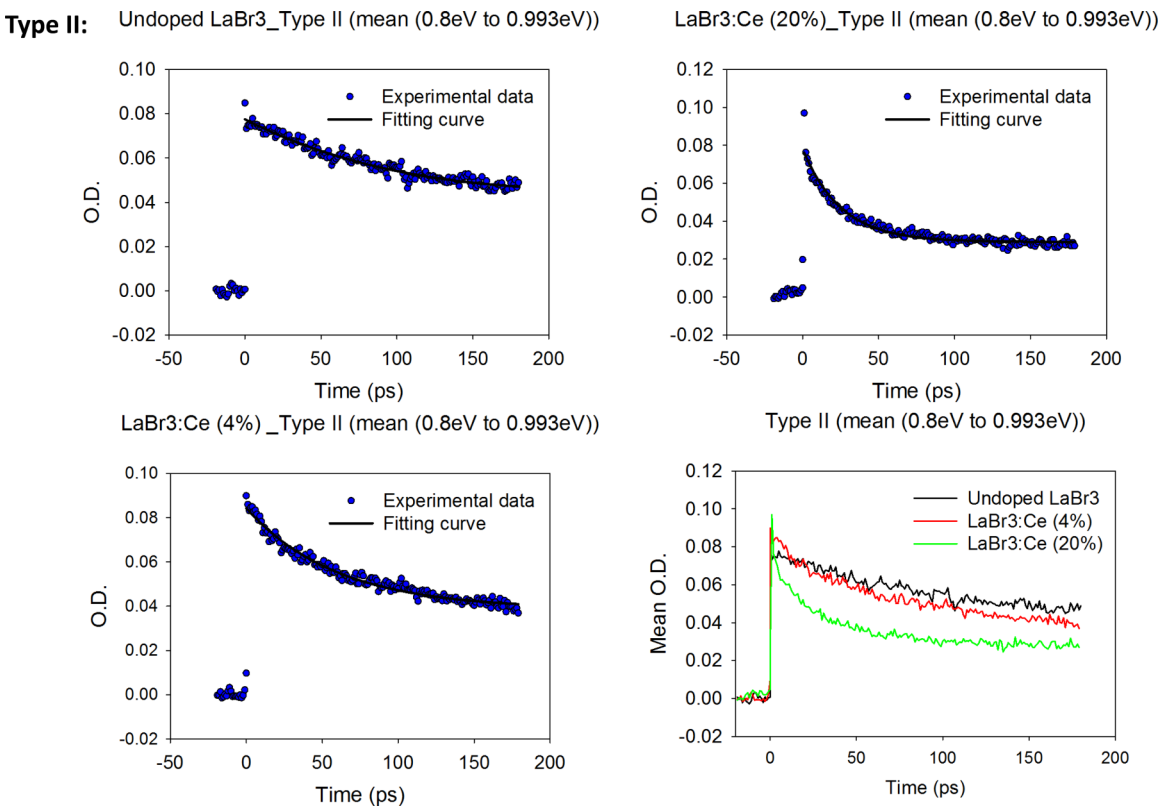

FIG. 16. Absorption at the wavelength range of type II STEs induced by second harmonic excitation is shown fitted by a single exponential decay and a constant, listed in Table II.

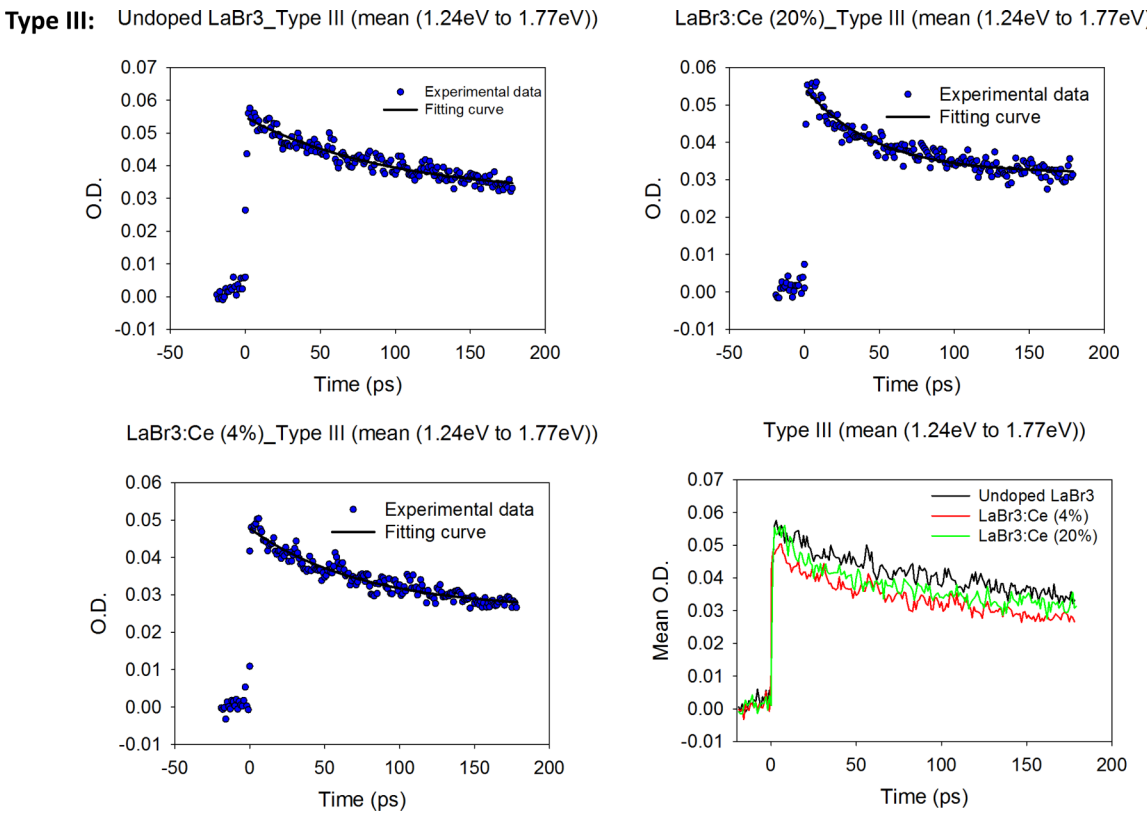

FIG. 17. Absorption at the wavelength range of type III STEs induced by second harmonic excitation is shown fitted by a single exponential decay and a constant, listed in Table II.

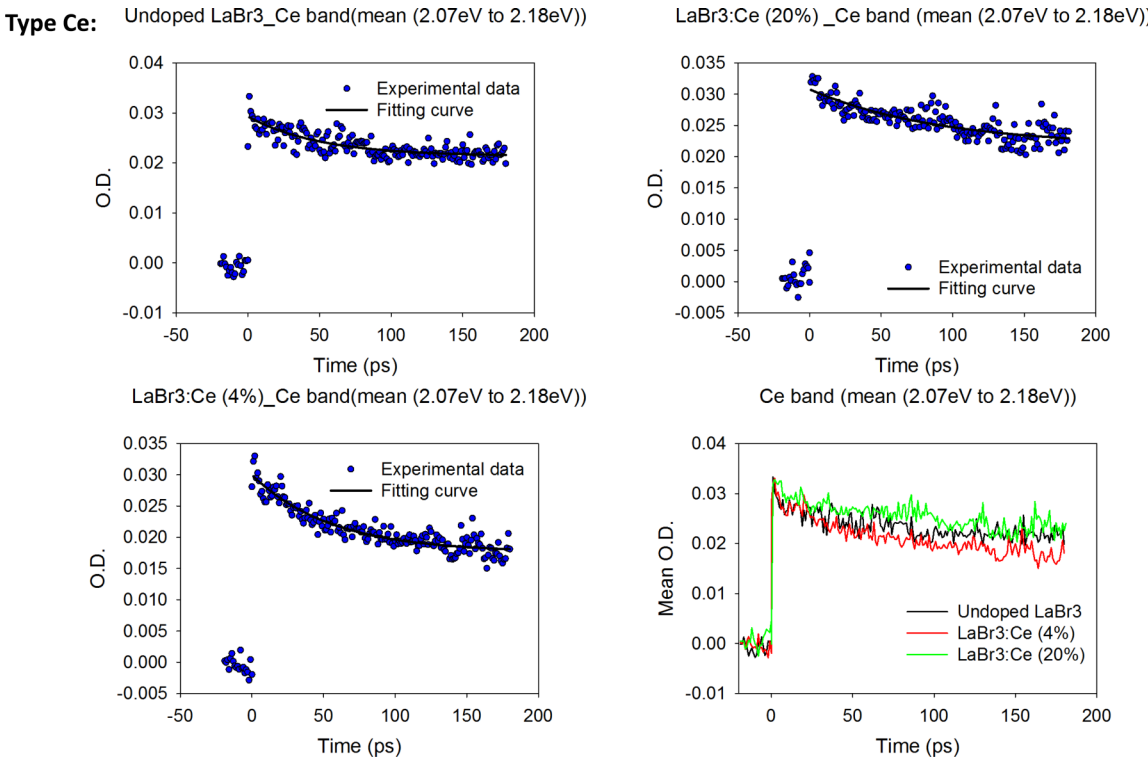

FIG. 18. Absorption at the wavelength range attributed to Ce^{3+*} induced by second harmonic excitation is shown fitted by a single exponential decay and a constant, listed in Table II.

We suggest that the fast STE decay in tens of picoseconds depending on Ce concentration is the prompt or "process I" transfer of STE energy to Ce^{3+*} in the terms of Bizarri and Dorenbos [17]. They defined process I as prompt sequential capture of a free hole and then an electron on Ce^{3+}, whereas we do not observe hole capture on Ce^{3+} in the fast (picosecond) time scale when the excitation is electron-hole pair production in the $LaBr_3$ host. Instead, we observe STEs created promptly in less than 1 picosecond and then decaying in tens of picoseconds presumably by energy transfer to Ce^{3+}. The STEs should decay primarily by energy transfer rather than quenching because $LaBr_3$:Ce is a very efficient scintillator. Tens of picoseconds appears instantaneous on the time scale of the luminescence measurements in Ref. [17], so we identify this picosecond transfer as their process I resulting in "initial" population of the Ce^{3+*} emissive state. We suggest that the physical mechanism of this tens-of-picoseconds energy transfer process is dipole-dipole transfer from STEs at the location of their first creation near a Ce^{3+} dopant. Near is defined as being within a sphere of radius R_{dd}, where R_{dd} is the characteristic Förster dipole-dipole transfer radius, typically of order 3 nm. The second-order rate constant of dipole-dipole transfer in a rate equation of form

$$\frac{\partial n_{\rm ex}}{\partial t}|_{\rm dipole\text{-}dipole} = -k_2(t)n_{\rm ex}^2, \tag{1}$$

can be expressed in the following form [43,44]:

$$k_2(t) = \frac{2}{3}\pi^{\frac{3}{2}}\frac{R_{dd}^3}{\sqrt{\tau_R}}\frac{1}{\sqrt{t}}. \tag{2}$$

The tens-of-picoseconds Ce-concentration dependent transfer rate should represent the average of transfer rates over multiple dipole-dipole distances consistent with the lattice structure and falling within the sphere of radius R_{dd}. The higher the Ce concentration, the more randomly created STEs on these sites will fall within R_{dd} of a given Ce, hence the fast-decaying STE fraction should become larger as observed in Table II. Furthermore, each STE will gain multiple dd transfer channels to different Ce neighbors at high Ce concentration. The decay rates to each neighboring Ce should add to give the effective decay rate of a given STE, hence the decay time of STE due to dipole-dipole transfer will become faster with increasing Ce concentration, as also seen in Table II. This trend agrees qualitatively with the dependence of Ce^* scintillation rise time on Ce concentration measured by Glodo et al [45].

TABLE II. Decay time, pre-exponential coefficient, and constant used to fit absorption (OD) decay to the function $OD = A\exp(-t/\tau) + B$, vs band type and Ce concentration in the sample.

Band	Doping	A	τ (ps)	B
I (0.48 eV)	undoped	0.037	80	0.051
I	4%Ce	0.037	72	0.027
I	20%Ce	0.060	42	0.031
II (0.8-0.99 eV)	undoped	0.037	99	0.041
II	4%Ce	0.046	60	0.039
II	20%Ce	0.049	25	0.029
III (1.24-1.8 eV)	undoped	0.024	97	0.031
III	4%Ce	0.022	74	0.026
III	20%Ce	0.023	47	0.032
Ce^* (2.1–2.2 eV)	undoped	0.008	50	0.021
Ce^*	4%Ce	0.012	55	0.018
Ce^*	20%Ce	0.010	90	0.022

The constant, B, in our fitting of the STE decay is assumed to represent a decay time in the nanoseconds range in these room temperature data. Bizarri and Dorenbos found that the room-temperature decay of Ce luminescence in Ce-doped $LaBr_3$ occurs with the 16-ns Ce^* radiative lifetime, implying that the "Process II" of thermally-activated STE transfer occurs in less than 16 ns. Detailed scintillation rise-time measurements in $LaBr_3$:Ce with fast coincidence methods by Glodo *et al.* [45] and Seifert *et al.* [46] have identified prompt and slower stages of scintillation rise for 5% Ce given as 380 ps [45] or 270 ps [46], and 2.2 ns [45] or 2.0 ns [46], respectively. We suggest that the ~300 ps rise reported in Refs. [45,46] corresponds to a limited-resolution measurement of what we identify as dipole-dipole transfer to Ce from STEs created in place (no thermal migration), and the ~2.1 ns process is the thermally activated process II at room temperature in a 5% Ce doped sample.

If we are correct in attributing the tens-of-picoseconds decay of STE to dipole-dipole transfer of the STE energy to create Ce^{3+*} excited states, and if we correctly identified the 2.1-eV absorption band in Figs. 7 and 9 as charge-transfer excitation out of Ce^{3+*} $5d$, then we should expect to see the 2.1 eV band in Figs. 6 and 8 as well, growing at a tens-of-picoseconds rate to match the decay of the STEs which are transferring energy. We do not see that closure of the loop clearly. There is not a distinct 2.1-eV band in Figs. 6 and 8. According to the false color legend, the blue color at 2.1 eV does not indicate zero induced absorption, but rather about 40% of the value induced there by third harmonic excitation. This indicates that the absorption observed in the region around 2.1 eV is created promptly on the scale of picoseconds upon host crystal excitations rather than growing at the rate of STE decay. This can be seen most clearly in the decay time plots of Fig. 13 and the amplitude coefficients in Table II. There are at least two circumstances that could produce this result and still be consistent with our above identifications of STE and Ce^{3+*} excited states. One is if STE absorption and the Ce^{3+*} absorption band overlie each other in the 2.1-eV range. The STE absorption is created suddenly and then partly decays with an exponential time constant τ. If it spectrally overlaps a band such as Ce^{3+*} that grows with the same time constant due to dipole-dipole transfer, and has equal strength, their sum would be a step function. If the strengths are not equal, there will be a smaller net decay or net growth relative to the step function. The plots of 2.1-eV absorption in Fig. 9 allow such an interpretation.

A second circumstance that could make the observation of growing Ce^{3+*} absorption after host excitation difficult is if the STE has an additional decay channel besides transfer to Ce. This could be thermal quenching since these measurements were made at room temperature. In that case the time constants for decay of STE and for growth of Ce^{3+*} would not be the same. Unfortunately, the thermal quenching rate of STEs in pure $LaBr_3$ has not been measured yet. If thermal quenching is significant at room temperature, the growth of Ce^{3+*} would be slower than the total decay rate of STE. Time constants

longer than 180 ps are difficult to measure with the delay line and optics in our experiment. Related to this, the luminescence rise data [17,45,46] indicate that there is a much slower 2.1-ns growth stage in Ce^{3+*} population at room temperature, likely attributable to thermally activated migration of STEs over some distance [17].

Coverage of the gap between picoseconds and multiple nanoseconds is being pursued in ongoing experimental work in which the sample is excited by 300-fs laser pulses as before, but induced absorption is measured with a xenon flashlamp and streak camera. Preliminary data of this kind shown in Fig. 14 suggest slower growth of the supposed Ce^{3+*} band at ~2.15 eV in 4% Ce-doped $LaBr_3$ at room temperature, compared to the growth of absorption at 2.37 and 2.62 eV. The 10%–90% rise times are 1, 0.62, and 0.5ns at 2.15, 2.37, and 2.62 eV spectral ranges, respectively, where ~0.5 ns rise may be attributed to trigger jitter of the streak camera.

IV. CONCLUSION

The following conclusions are drawn from the results presented. (1) A V_k-type ultraviolet band is found in $LaBr_3$ and $LaBr_3$:Ce when interband excitation of the host $LaBr_3$ is accomplished by two-photon absorption. A supporting corollary to this is that when the excitation pulse wavelength causes it to be absorbed directly on Ce rather than two-photon excitation of the host, the V_k-type ultraviolet band is not found. Since the V_k-type band is found in both undoped $LaBr_3$ and Ce-doped $LaBr_3$, and furthermore since Ce^{3+} in $LaBr_3$ is widely considered not to be an electron trap, we conclude that the observed UV band is probably the $\sigma_u \rightarrow \sigma_g$ hole transition of self-trapped excitons rather than of bare self-trapped holes (V_k). Finding a V_k-like hole transition of the STE in transient optical absorption of $LaBr_3$ is not unexpected, since existence of STEs in this material has been well established by observations of STE luminescence [17] and optically-detected EPR in the similar material $LaCl_3$ [7]. Furthermore, calculations by Canning and del Ben have reproduced the Br_2^- based structures of both STHs and STEs in $LaBr_3$ [8]. This report is the first study of excitation-induced transient (picosecond) optical absorption in $LaBr_3$ without and with Ce doping, and it finds the absorption signature expected for a $(Br_2)^-$ based STE hole transition.

(2) The bound-electron absorption bands of the self-trapped exciton have been observed and identified in the red/infrared spectrum. Their identification and classification as on-center, weakly off-center, and strongly off-center (types I, II, III) was facilitated by similarities to corresponding observations in the well-studied alkali halides. The theoretical calculations of Canning et al also found on-center, weakly off-center, and strongly off-center configurations of STEs in $LaBr_3$ [8].

(3) Self-trapped excitons are the dominant species observed to be produced by interband excitation of electron-hole pairs in the host $LaBr_3$, even when Ce dopant is present. This finding is consistent with the main part of the STE-transport based model previously proposed by Bizarri and Dorenbos [17] to account for their observations on STE and Ce* gamma-excited luminescence (scintillation) in $LaBr_3$ with different Ce concentrations and at different temperatures. Their luminescence measurements were on ~1 ns and longer time scales, whereas the present induced absorption measurements are on the 0.5 to 180 ps time scale. Alternative species such as holes promptly trapped on Ce^{3+} (forming Ce^{4+}), promptly excited cerium, Ce^{3+*}, or electrons trapped on a recognizable defect or activator site were not found in any significant number in the first 180 ps when electron-hole pairs in the $LaBr_3$ host crystal were being excited. Rather than prompt Ce^{4+} formation by hole capture followed by electron capture to create excited Ce^{3+*} corresponding to the "prompt process I" suggested in Ref. [17], we observe STE formation in <1 ps and partial decay in tens of picoseconds attributed to dipole-dipole energy transfer to Ce. Our 5.9-eV two-photon interband excitation of the $LaBr_3$ produces electrons and holes near the band edges, which could favor STE formation relative to the hotter carriers produced by gamma rays. However, 8.83-eV excitation of hot carriers in the undoped $LaBr_3$ also indicates STE formation within a picosecond. It is important to link and correlate the two kinds of data and the two not-quite-overlapping time scales in this study and in Ref. [17]. We are making a start on that in some of the discussion to follow.

(4)As observed particularly in their bound-electron absorption spectra, self-trapped excitons are formed at their maximum population within less than 1 ps of e-h pair generation, and very roughly 50% of them (the fraction varying with Ce concentration) decay with time constants of tens of picoseconds, also depending on Ce concentration. The behavior was summarized in the fitting coefficients of Table II. This fast decay of STEs probably occurs by energy transfer to Ce^{3+} because $LaBr_3$:Ce has a very high light yield, which would be inconsistent with losing the observed ~50% fraction of fast decaying STEs to a decay channel other than Ce^{3+*} production. Furthermore, the STE decay rate increases with higher Ce concentration so the decay rate of STE is somehow linked to the presence of Ce dopant. Tens of picoseconds is instantaneous on the time scale of the luminescence measurements in Ref. [17], so this transfer qualifies as part or all of the prompt Ce^{3+*} production that they observed and labeled as process I. We suggest that the physical mechanism of this tens-of-picoseconds energy transfer process is dipole-dipole transfer from STEs at the location of their first creation close to a Ce^{3+} ion, so that no thermally activated migration of the STE is required. The tens-of-picosecond Ce-concentration dependent transfer rate should represent the average of transfer rates over multiple dipole-dipole distances consistent with the lattice structure and falling within a sphere of radius R_{dd}. The higher the Ce concentration, the higher the probability that randomly created STEs will fall within R_{dd} of a given Ce. Hence the fast-decaying STE fraction should become larger with increased Ce concentration, as observed. Furthermore, each STE will gain multiple diple-dipole transfer channels to different Ce neighbors at high Ce concentration. The decay rates to each neighboring Ce should add to give a faster decay time with increasing Ce concentration. Fast photon coincidence measurements have shown that the scintillation risetime in $LaBr_3$:Ce decreases significantly with increasing Ce concentration, from 9 to 0.16 ns as [Ce] goes from 0.5% to 20% [45]. This supports the conclusion above.

(5) The constant in our fitting of the STE decay is assumed to represent the amplitude of a decay component in the nanoseconds range in these room temperature data. Bizarri and Dorenbos found that the room-temperature decay of Ce

luminescence in Ce-doped $LaBr_3$ matches the 16-ns radiative lifetime of excited Ce^*, implying that the process II of thermally-activated STE transfer occurs in less than 16 ns at room temperature. Detailed scintillation rise-time measurements in $LaBr_3$:Ce with fast coincidence methods by Glodo *et al.* [45] and Seifert *et al.* [46] have identified a fast stage and a slower stage of scintillation rise reported as ∼300 ps and ∼2.1 ns, respectively. We suggest that the ∼300 ps rise corresponds within the time resolution of the measurement to what we identified in No. 4 above as dipole-dipole transfer to Ce from STEs created in the close neighborhood, and that the 2.1-ns process is the thermally activated slow process II at room temperature in 5% Ce-doped $LaBr_3$. Slow process II was described in Ref. [17] as the thermal migration of STE over a distance to encounter a Ce dopant.

(6) In addition, the experiments of Ref. [17] at lower temperature and lower Ce concentrations revealed evidence of a "fast process II" that was thermally activated with a different activation energy than was measured for the "slow process II" attributed to migration of STEs over some distance. They proposed that fast process II is a thermally activated process governing the rate of the final step in energy transfer from STEs to Ce after STEs reach the near-neighborhood of Ce. The existence of thermal activation of STE-to-Ce energy transfer at close range, which is distinct from thermally activated diffusion of STEs at long range was indicated by the temperature-dependent data in Ref. [17]. It is an intriguing concept. We can suggest two possible physical origins for the effect, which may be amenable to testing upon future completion of low-temperature picosecond absorption spectroscopy. The two possible mechanisms we suggest for fast process II temperature dependence are summarized as follows.

(a) Resonant transfer of energy from the STE luminescent state in $LaBr_3$ to the emissive Ce^{3+*}(5d) state is already on the verge of being energetically problematic as an uphill transfer. Some overlap of the emission band of the energy-donor and the absorption band of the energy-acceptor is required for dipole-dipole transfer. The peak of the $LaBr_3$ STE emission band at 125 K is at 440 nm (2.8 eV) and its high-energy wing barely extends to 4 eV at 125 K [17]. The threshold of Ce^{3+}(4f-5d) absorption is about 4 eV at 10 K [24]. The temperature-dependent increase of dipole-dipole transfer rate due to thermally enhanced overlap of the STE emission and Ce($4f$-$5d$) absorption bands could be the fast process II that was observed [17]. STE emission bands typically retain a significant spectral width at low temperature because of their steep dissociative ground-state potential curve. It is therefore reasonable to expect a finite emission/absorption overlap at 4 eV to persist independent of temperature at low temperatures. The dipole-dipole transfer rate is proportional to emission/absorption overlap [43,44,47]. To play with labels a bit, the temperature-independent "prompt" and temperature-dependent "II_{Fast}" processes observed by Bizarri and Dorenbos [17] could be the temperature-independent and temperature-dependent terms in STE/Ce^{3+} emission/absorption overlap determining dipole-dipole transfer rate.

(b) The rate of dipole-dipole transfer scales as $(1/r_{dd})^6$, where r_{dd} is the (variable) distance between the two dipoles, in this case STE and Ce [43,44,47]. Now imagine that just a single thermally activated hop of the STE occurs. In some cases, the hop will increase r_{dd}, and in those cases the transfer is suppressed. But in other cases, the hop decreases r_{dd}, and because of the strong inverse sixth power dependence, the transfer rate in that case becomes much faster because of a single hop of the order of a lattice constant. We have suggested that the temperature-independent prompt process I is mainly the dipole-dipole transfer rate averaged over the r_{dd} distances corresponding to sites of STE creation in the lattice. The average r_{dd} decreases with increasing Ce concentration, so both the fraction of STEs participating in the transfer and the average rate of transfer increase correspondingly. Then if the temperature is such that STEs can make a hop before they decay by other paths, there will be additional dipole-dipole transfers because of the hops to closer r_{dd} as outlined above. This might be an alternative reason for the fast process II. The activation energy and/or pre-exponential factor would have to be different for these STE hops in the near neighborhood of Ce compared to STE migration over a distance in order to agree with the experiments in Ref. [17]. That has not been tested yet.

(7) When exciting Ce^{3+} directly with an intense pulse of 4.43-eV light (third harmonic of our laser), a strong new band is seen at 2.1 eV, becoming stronger as Ce concentration increases. For reasons detailed below Figs. 10 and 11, we tentatively assign the 2.1 eV absorption band to electron excitation from the Ce^{3+*} ($4f$-hole, $5d$-electron) excited dopant into the conduction band. Therefore 2.1-eV absorption is a useful signature of the population of the Ce^* excited states that are responsible for scintillation in $LaBr_3$:Ce. If correctly assigned, this absorption signature of luminescent Ce^* excited states can be measured on faster (picosecond and subpicosecond) time scales than can the scintillation itself by typically used methods. We have presented in Fig. 14 preliminary absorption results excited by the subpicosecond laser pulse but probed by a xenon flashlamp and streak camera in an effort to bridge the time gap between picosecond absorption and the existing fast scintillation data. The medium-fast (subnanosecond and nanosecond) range of absorption and emission data under subpicosecond laser excitation will be studied more in future work.

(8) We observed very short-lived absorption bands resembling STE bound-electron spectra upon the direct excitation of Ce by a 4.43-eV laser pulse capable of driving two- and three-photon transitions on Ce assisted by real intermediate states, namely the Ce^{3+} empty $4f$ and filled $5d$ levels. As was illustrated in Fig. 12, a three-step excitation of Ce^{3+} could result in production of an electron-hole pair immediately adjacent to a Ce^{3+} ion in its ground state, which could then form an STE immediately adjacent to Ce^{3+}. We suggest that this is the origin of the very short-lived STE bands seen in the third harmonic experiments on Ce-doped samples. Furthermore, their ∼1 ps decay time seen in Figs. 7 and 9 could be the direct observation of dipole-dipole transfer from the closest STE site adjacent to Ce^{3+}. Interestingly, D. L. Dexter evaluated the dipole-dipole transfer time at the distance between two closest positive ions in NaCl (0.397 nm) for assumed good overlap of absorption and emission, finding $\tau \approx 0.1$ to 1 ps [47]. For moderately poor overlap in $LaBr_3$ as discussed in conclusion 1(a), the 1-ps upper limit of Dexter's 1953 estimate seems spot-on. In the same experiment that shows 1-ps decay of the STE adjacent to Ce, the 2.1 eV absorption band attributed to Ce^{3+*} is seen to be formed within 1 ps.

In summary, intrinsic relaxed electronic excited states in pure alkali mono-halide, alkaline-earth di-halide, and lanthanum trihalide compounds have now been characterized in all the three material classes by transient optical absorption. This complements previous x-ray-excited luminescence and optically detected EPR studies as well as first-principles calculations of the relaxed excited states in these three compound classes. Several observations common to the studied members of all three compound classes can be recognized. Holes self-trap in a V_k-type halide pair configuration in all three materials, and electrons and holes form self-trapped excitons within about 1 ps. Further optical excitations of the STE can be seen as transient absorption bands that divide into an ultraviolet hole band and infrared or visible bound-electron transitions of roughly similar form in all three compound classes. Presence of the bound electron in the STE causes the halide pair bearing the hole in an initially V_k-like configuration to translate and/or rotate to one or more (typically three) relaxed configurations in which the halide pair is displaced. The STH and STE are mobile by thermal activation, and can in that way transport charge (STH) or energy (STE). In alkali halides doped with thallium, specifically NaI:Tl and CsI:Tl, it has been shown that energy is transported mainly by separated charges, i.e., STH and electrons trapped on Tl [21,22,48]. The present study confirms the conclusion of Bizarri and Dorenbos that energy transport in $LaBr_3$:Ce proceeds mainly by STE [17]. This difference between the recombination physics in alkali halide and lanthanum halide scintillators seems to follow from the properties of the dopants: Tl^+ in alkali iodides is an excellent trap for both electrons and holes, so its presence actually suppresses STE formation by out-competing the STH for initial electron capture [21–23,48], whereas Ce^{3+} in lanthanum bromide is apparently not an electron trap. At least in our experiments with laser interband excitation, self-trapped holes in $LaBr_3$ appear to be better at capturing electrons than Ce^{3+} ions are at capturing holes. For one reason, the STH is a coulombic electron trap from a distance, whereas substitutional Ce^{3+} in $LaBr_3$ is a neutral trap (at best) for either carrier. The result seems to be that STEs are created first before substantial excitation of Ce^{3+} or formation of Ce^{4+}. The present study indicates that dipole-dipole transfer of energy from STE to Ce^{3+} is very effective in $LaBr_3$:Ce despite their rather poor emission/absorption overlap, with transfer time of 1 ps from an adjacent lattice site and ∼30 to 90 ps when averaged over a number of close sites. Thermal broadening of STE emission and Ce^{3+} absorption bands should increase STE/Ce emission/absorption overlap and may thereby produce the observed temperature-dependent "fast process II of energy transfer."

ACKNOWLEDGMENTS

The WFU authors acknowledge support from Saint-Gobain Crystals and from the National Nuclear Security Administration (NNSA), Office of Defense Nuclear Nonproliferation Research and Development (DNN R&D) LB15-V-GammaDetMater-PD2Jf, under subcontract from Lawrence Berkeley National Laboratory. We thank K. Yang, P. Dorenbos, G. A. Bizarri, E. D. Bourret, A. Canning, D. R. Onken, and D. Aberg for helpful discussions, and A. Canning and M. del Ben for sharing theoretical results prior to publication. We thank G. Donati and acknowledge NSF major instrumentation grant CHE-1531698 for ICP-MS used to measure Ce trace concentration in the undoped $LaBr_3$, and Saint-Gobain (France) for ICP-AES on the other samples.

[1] W. Känzig, Phys. Rev. **99**, 1890 (1955).
[2] W. Hayes and J. W. Twidell, Proc. Phys. Soc. **79**, 1295 (1962).
[3] R. T. Williams and M. N. Kabler, Phys. Rev. B **9**, 1897 (1974).
[4] R. T. Williams, J. N. Bradford, and W. L. Faust, Phys. Rev. B **18**, 7038 (1978).
[5] K. S. Song and R. T. Williams, *Self-Trapped Excitons*, Springer Series in Solid-State Sciences Vol. 105 (Springer, Berlin, Heidelberg, 1993).
[6] R. T. Williams, M. N. Kabler, W. Hayes, and J. P. Stott, Phys. Rev. B **14**, 725 (1976).
[7] U. Rogulis, S. Schweizer, J.-M. Spaeth, E. V. D. Van, P. Dorenbos, C. W. E. Van Eijk, K. Kramer, and H. U. Gudel, Radiat. Eff. Defects Solids **157**, 951 (2002).
[8] A. Canning and M. del Ben (private communication).
[9] E. V. D. van Loef, P. Dorenbos, C. W. E. van Eijk, K. Krämer, and H. U. Güdel, Appl. Phys. Lett. **79**, 1573 (2001).
[10] A. Favalli, H.-C. Mehner, V. Ciriello, and B. Pedersen, Appl. Radiat. Isot. **68**, 901 (2010).
[11] A. Kuhn, S. Surti, J. Karp, P. Raby, K. Shah, A. Perkins, and G. Muehllehner, IEEE Trans. Nucl. Sci. **51**, 2550 (2004).
[12] C. Stoller, B. Adolph, M. Berheide, T. Brill, P. Clevinger, S. Crary, B. Crowder, S. Fricke, J. Grau, M. Hackbart, S. Herron, B. Jorion, M. Lorente, D. Madio, J. Miles, O. Philip, R. J. Radtke, B. Roscoe, I. Shestakova, W. Ziegler, and P. R. Menge, in *2011 IEEE Nuclear Science Symposium Conference Record, Valencia, Spain* (IEEE, Washington, DC, 2011), pp. 191–195.
[13] P. Dorenbos, IEEE Trans. Nucl. Sci. **57**, 1162 (2010).
[14] https://www.crystals.saint-gobain.com/products/brillance-labr3-lanthanum-bromide.
[15] K. Yang, P. R. Menge, J. J. Buzniak, and V. Ouspenski, in *2012 IEEE Nuclear Science Symposium and Medical Imaging Conference Record (NSS/MIC), Anaheim, CA, USA* (IEEE, Washington, DC, 2012), pp. 308–311.
[16] M. S. Alekhin, D. a. Biner, K. W. Krämer, and P. Dorenbos, J. Appl. Phys. **113**, 224904 (2013).
[17] G. Bizarri and P. Dorenbos, Phys. Rev. B **75**, 184302 (2007).
[18] E. V. D. van Loef, P. Dorenbos, and C. W. E. van Eijk, J. Phys.: Condens. Matter **15**, 1367 (2003).
[19] A. Bessiere, P. Dorenbos, C. van Eijk, K. Kramer, H. Gudel, C. de Mello Donega, and A. Meijerink, Nucl. Instrum. Methods Phys. Res., Sect. A **537**, 22 (2005).
[20] D. Wu, M. P. Prange, F. Gao, and S. Kerisit, J. Lumin. **176**, 227 (2016).
[21] X. Lu, Q. Li, G. A. Bizarri, K. Yang, M. R. Mayhugh, P. R. Menge, and R. T. Williams, Phys. Rev. B **92**, 115207 (2015).
[22] X. Lu, S. Gridin, R. T. Williams, M. R. Mayhugh, A. Gektin, A. Syntfeld-Kazuch, L. Swiderski, and M. Moszynski, Phys. Rev. Appl. **7**, 014007 (2017).
[23] K. B. Ucer, G. Bizarri, A. Burger, A. Gektin, L. Trefilova, and R. T. Williams, Phys. Rev. B **89**, 165112 (2014).

[24] P. Dorenbos, E. van Loef, A. Vink, E. van der Kolk, C. van Eijk, K. Krämer, H. Güdel, W. Higgins, and K. Shah, J. Lumin. **117**, 147 (2006).
[25] V. A. Pustovarov, V. Y. Ivanov, A. N. Razumov, and D. I. Vyprintsev, IOP Conf. Ser.: Mater. Sci. Eng. **49**, 012047 (2013).
[26] E. D. Thoma, H. M. Yochum, and R. T. Williams, Phys. Rev. B **56**, 8001 (1997).
[27] H. Nishimura, J. Phys. Soc. Jpn. **52**, 3233 (1983).
[28] H. Nishimura, C. Ohhigashi, Y. Tanaka, and M. Tomura, J. Phys. Soc. Jpn. **43**, 157 (1977).
[29] C. J. Delbecq, W. Hayes, and P. H. Yuster, Phys. Rev. **121**, 1043 (1961).
[30] A. N. Jette, T. L. Gilbert, and T. P. Das, Phys. Rev. **184**, 884 (1969).
[31] R. T. Williams, K. S. Song, W. L. Faust, and C. H. Leung, Phys. Rev. B **33**, 7232 (1986).
[32] K. ichi Kan'no, K. Tanaka, H. Kosaka, T. Mukai, Y. Nakai, M. Itoh, T. Miyanaga, K. Fukui, and M. Watanabe, Phys. Scr. **41**, 120 (1990).
[33] D. Block, A. Wasiela, and Y. M. D'Aubigne, J. Phys. C **11**, 4201 (1978).
[34] K. Edamatsu, M. Sumita, S. Hirota, and M. Hirai, Phys. Rev. B **47**, 6747 (1993).
[35] H. Nishimura, M. Sakata, T. Tsujimoto, and M. Nakayama, Phys. Rev. B **51**, 2167 (1995).
[36] P. Dorenbos, J. Lumin. **136**, 122 (2013).
[37] P. Dorenbos, Phys. Rev. B **85**, 165107 (2012).
[38] P. Dorenbos, J. Phys.: Condens. Matter **25**, 225501 (2013).
[39] S. Blahuta, A. Bessiére, B. Viana, P. Dorenbos, and V. Ouspenski, IEEE Trans. Nucl. Sci. **60**, 3134 (2013).
[40] D. Åberg, B. Sadigh, and P. Erhart, Phys. Rev. B **85**, 125134 (2012).
[41] S. Sato, J. Phys. Soc. Jpn. **41**, 913 (1976).
[42] W. Setyawan, R. M. Gaume, R. S. Feigelson, and S. Curtarolo, IEEE Trans. Nucl. Sci. **56**, 2989 (2009).
[43] A. Vasil'ev, IEEE Trans. Nucl. Sci. **55**, 1054 (2008).
[44] A. N. Vasil'ev and V. V. Mikhailin, *Principles of Insulator Spectroscopy* (Moscow State University, Moscow, Russia, 2010) translated from Russian.
[45] J. Glodo, W. Moses, W. Higgins, E. van Loef, P. Wong, S. Derenzo, M. Weber, and K. Shah, IEEE Trans. Nucl. Sci. **52**, 1805 (2005).
[46] S. Seifert, J. H. L. Steenbergen, H. T. van Dam, R. Vinke, P. Dendooven, H. Lohner, F. J. Beekman, P. Dorenbos, E. van der Kolk, and D. R. Schaart, in *IEEE Nuclear Science Symposuim & Medical Imaging Conference, Knoxville, TN, USA* (IEEE, Washington, DC, 2010), pp. 1736–1739.
[47] D. Dexter, J. Chem. Phys. **21**, 836 (1953).
[48] H. Dietrich, A. Purdy, R. Murray, and R. Williams, Phys. Rev. B **8**, 5894 (1973).